



Sudan University of Science and Technology

College of Graduate Studies



**Determination of the Optical, Nano, and Acidity Properties'
for Water and Blood Preservation Using Different
Concentrations of Tio₂**

**تحديد الخواص الضوئية والنانوية والحمضية لمعالجة الماء وحفظ الدم
بتركيزات مختلفة من ثاني أكسيد التيتانيوم**

**A thesis Submitted for Fulfillment of Requirements for
Degree of Doctor of Philosophy in Physics**

By

HIBA MIN AHA ELOBEID GIBREEL

Main Supervisor: Prof: Mubarak Dirar Abdalla

C- Supervisor: Dr: Ahmed AL Hassan Alfaki

August 2021

بِسْمِ اللَّهِ الرَّحْمَنِ الرَّحِيمِ

((ولكل وجهة هو موليها فاستبقوا الخيرات أين
ما تكونوا يأت بكم الله جميعا إن الله على كل
شيء قدير))

صدق الله العظيم

سورة البقرة الآية 148

Dedication

I dedicate this modest research to my father,

The one who inspires in me the spirit of achievement.

To my beloved mother, Insaf Muhammad NoorAlhassan,

The candle that lights the way for me.

to my dear loving husband, Saeed Muhammad Elobeid,

The main given of assistance and encouragement to me.

**to my brother Abu-Bakr and sisters, Manal, Negate, Selma, Amina,
Amal**

to the little sweet birds of the garden of my family:

Retaj, Muhammad, Majdi, Rama, Jinan, Habib, Amina and Awab.

to all my intimate friends and dear classmates.

My relative and previous teacher nuclear physics.

And Acknowledgment to Very Important Dr' Abdul shake Suleiman

Acknowledgement

Praise and thanks are due to Allah who had given me the Power and Patience to complete this Work. I would like to thank the members of our department for their assistance in many ways. I am thankful and grateful to my Main Supervisor prof. Mubarak Dirar Abdulla, Sudan University for Science and Technology, and grateful and special thanks to my Family for their help, Valuable suggestions, and unlimited help throughout this study. Deep thanks are also extended to my Co-Supervisor Dr. Ahmed Al Hassan Alfaki and Dr. Abdul Shake Suleiman also for all professors of the department of physics faculty of Science and technology. I am thankful thankful and testimonial to my husband Saeed Mohammed. I would like to thank the members of our department for their assistance.

Abstract

The Physical Properties of blood and water plays an important role in human health and killing germs and killing germs. Motivated by the role of TiO_2 in changing ultraviolet absorption which kill germs, the aim of this work is to see how adding TiO_2 with different concentrations to both blood and water affect their absorption, PH and other related properties to do this TiO_2 having concentrations 0.1, 0.2, 0.3, 0.4, 0.5, 0.6, 0.7 and 0.8. Ppm were added to blood and water respectively. Titanium dioxide (TiO_2) Nano structure was also determined using X-ray diffraction (XRD) apparatus and scanning electron microscope (SEM). The XRD result shows Nano crystal size ranging from about 45 to 60 nm. However the SEM result shows wider range from about

60-200 nm. This difference may be attributed to the fact that XRD technique allows only determination of sizes in every narrow region where the rays are incident, while SEM image cover the whole surface. The ultra violet (UV) test of TiO_2 how's energy gap of 3.773 eV. For the 8 blood samples (with TiO_2 concentrations 0.1, 0.2, 0.3, 0.4, 0.5, 0.6, 0.7 and 0.8 ppm) UV absorption and the count rate of red and white blood cells (RBC and WBC) beside hematocrit (HCT) were found for difference concentrations and when the eight blood samples immediately (examined) in the first week then the second, third and fourth week. The UV results indicates decrease of blood absorption up on increasing TiO_2 concentration, and increase of absorption with time. The HCT

Which is directly proportional to the viscosity, it decreases up on increasing TiO_2 concentration, an also decreases with time. The RBC count rate decreases up on increasing TiO_2 concentration an increasing and increasing time except slight increase in the fourth week. The WBC count rate decreases in the TiO_2 concentration range (0.1-0.6) up on increasing concentration in the range (0.7-0.8) with concentration, but count rate decreases with time.

For water 8 samples were also prepared for TiO_2 concentrations (0.1, 0.2, 0.3, 0.4, 0.5, 0.6, 0.7 and 0.8 ppm). The pH and the number of living cells of *Escherichia coli* for each sample were determined. The results obtained show that water pH decreases upon increasing TiO_2 concentration and with time also. The number of living cells decreases upon increasing TiO_2 concentration and also with time. This means that increasing water pH increases the number of living cells.

المستخلص

تلعب الخواص الفيزيائية للدم والماء دوراً مهماً في صحة الانسان وقتل الجراثيم. متشجعين بدور ثاني أكسيد التيتانيوم (TiO_2) في تغيير إمتصاصية الأشعة فوق البنفسجية التي تقتل الجراثيم، هدف هذا العمل لرؤية كيف تؤدي إضافة (TiO_2) بتركيزات مختلفة للدم والماء معاً للتأثير على الإمتصاصية والأس الأيدروجيني (PH) وبعض الخواص الأخرى ذات الصلة. لعمل ذلك إضيف ثاني أكسيد التيتانيوم (TiO_2) بتركيزات (0.1, 0.2, 0.3, 0.4, 0.5, 0.6, 0.7 and 0.8 PPM) الى الدم والماء بالترتيب. ثم تحديد التركيب النانوي لثاني أكسيد التيتانيوم (TiO_2) بإستخدام جهاز حيود أشعة X (XRD) وجهاز المجهر الإلكتروني الماسح (SEM). بينت نتيجة (XRD) أن الحجم النانوي للبلورات يتراوح بين حوالي 40 إلى 60 نانو متر (nm) بيد أن نتيجة (SEM) أظهرت نطاقاً أوسع يتراوح ما بين حوالي 60 إلى 200 نانو متر (nm). هذا الإختلاف ربما يعزى لكون أن تقنية (XRD) تسمح بتحديد أبعاد في حيز ضيق جداً حيث تسقط الأشعة، في حين أن صورة (SEM) تغطي كل السطح. أما إختبار الأشعة فوق البنفسجية (UV) لـ TiO_2 فقد بين أن فجوة الطاقة تساوي 3.773 إلكترون فولت (ev). بالنسبة لعينات الدم الثمانية (بتركيزات TiO_2 : 0.1, 0.2, 0.3, 0.4, 0.5, 0.6, 0.7 and 0.8 ppm) فإن امتصاصية UV ومعدل عدد كريات الدم الحمراء والبيضاء (WBC, RBC) بجانب الهيماتوكرين (HCT) قد وجودوا للتركيزات المختلفة لـ TiO_2 وعند إختبار العينات الثمانية فوراً في الأسبوع الاول يليه الثاني والثالث والرابع. وقد بينت نتائج UV إنخفاض إمتصاصية الدم بزيادة تركيز TiO_2 وزيادة الإمتصاصية مع الزمن. بالنسبة للـ HCT التي تتناسب طردياً مع اللزوجة فقد تناقصت بزيادة تركيز TiO_2 وكذلك تناقصت مع الزمن. أما معدل عد (RBC) فتناقص بزيادة تركيز TiO_2 مع الزمن فيما عدا الزيادة الطفيفة التي حدثت في الأسبوع الرابع. فيما يخص معدل عد (WBC) فهي تناقصت في مدى تركيز TiO_2 (0.6 ppm – 0.1) مع زيادة التركيز في حين تزايدت في المدى (0.7 – 0.8) مع زيادة التركيز. بالنسبة لعينات الماء الثمانية فهي قد حضرت لتركيزات TiO_2 (0.1, 0.2, 0.3, 0.4, 0.5, 0.6, 0.7 and 0.8 ppm). تم تحديد ومعرفة الأس الأيدروجيني (PH) وعدد الخلايا (المستمرات) الحية للبركتريا أكلوي (*Escherichia coli*) لكل عينة. بينت النتائج المتحصل عليها نقصان PH بزيادة تركيز TiO_2 ومع الزمن أيضاً. أما عدد المستمرات الحية فتناقصت بزيادة تركيز TiO_2 ومع الزمن أيضاً. هذا يعني أن زيادة PH تزيد عدد المستمرات الحية.

Table of Contents

N0	Subject	Page
1	Holly Quran	I
2	Dedication	Ii
3	Acknowledgement	Iii
4	Abstract	Iv
5	Abstract(Arabic)	V
6	Index	Vi
7	Figures	Vii
8	Tables	Ix
	Chapter One Introduction	
1.1	Introduction	1
1.2	Research Problem	2
1.3	Aim of the work	2
	Chapter Two Theoretical background	
2.1	Introduction	4
2.2	Titanium dioxide	5
2.3	TiO₂ as Photo Catalysis	6
2.4	Synthetic Methods	9
2.5	Optical Parapets	10
2.5.1	Absorption	10
2.5.2	Transmission	10
2.5.3	Absorption coefficients	11
2.5.4	Reflection	12
2.5.5	Refractive index	12
2.5.6	Determination of Band Gaps	13
2.6	Human Blood	14
2.6.1	White Blood Cell count (WBC)	14
2.6.2	Red Blood Cell count(RBC)	15
2.6.3	Platelets (PLT)	16
2.6.4	Hemoglobin (HGB)	17
2.6.5	Hematocrit (HCT)	18

2.6.6	Mean Corpuscular Volume (MCV)	18
2.6.7	Mean Corpuscular Hemoglobin (MCH)	18
2.6.8	Mean Corpuscular Hemoglobin Concentration (MCHC)	18
2.6.9	Optical properties of blood	18
2.7	Wastewater Treatment	19
2.8	Literature Review	21
	Chapter Three Experimental Work	
3.1	Introduction	29
3.2	Material	29
3.2.1	Titanium Isopropoxide	29
3.2.2	Acetic Acid	30
3.2.3	Ethanol	31
3.3	Methods	32
3.4	Apparatus	32
3.4.1	Ray diffraction (XRD)	32
3.4.2	Infrared spectroscopy (FTIR)	34
3.5	Ultraviolet-visible spectrophotometer	35
3.6	Experiential one Synthesis and Cractraiztion TiO₂ Nanomaterial	36
3.7	The effect of adding TiO₂ nanomaterial to the blood samples	37
3.8	The effect of adding TiO₂ to water on its physical properties	37
	Chapter Four Results and Discussion	
4.1	Introduction	39
4.2	Results	39
4.2.1	Optical Results of TiO₂ sample	39
4.2.2	SEM Results of TiO₂ sample	42
4.2.3	XRD Results of TiO₂ sample	43
4.2.4	FTIR Results of TiO₂ sample	45
4.2.5	Blood and TiO₂ Results	46
4.2.6	Escherichia E.coli water and TiO₂ Results	53
4.3	Discsuasion	62
4.4	Conclusions	63
4.5	Future work	63
4.6	References	64

Content of Table

No	Subject	Page
2.1	Optical properties of human blood.	18
4.1	Lattice Constants from Peak Locations and Miller Indices [Tetragonal] of TiO₂ sample.	44
4.2	Parameters of T iO₂ sample.	45
4.3	Absorption curves riding statically of blood sample by different concentration of TiO₂ at First week.	46
4.4	Absorption curves riding statically of blood sample by different concentration of TiO₂ at Second week.	48
4.5	Absorption curves riding statically of blood sample by different concentration of TiO₂ at 3red week	49
4.6	Absorption curves riding statically of blood sample by different concentration of TiO₂ at Last week	51
4.7	Clinical examination of blood sample by different concentration of TiO₂	52
4.8	The effect of TiO₂ on the survival of number of viable cells Escherichia coli (CFU/ml) after 4 weeks on the water	57
4.9	Change of water PH with Tio₂ concentration and time.	60

Content of Figures

No	Subject	Page
2.1	The principle of water splitting using a semiconductor photo catalyst.	7
2.2	White Blood Cell count (WBC) [23].	15
2.3	Red Blood Cell count(RBC) [23].	16
2.4	Platelets (PLT) [24].	17
3.1	Schematic X-ray diffract meter of the Bragg-Brentano type.	33
3.2	Continuous Wave spectrometers (FTIR).	34
3.3	UV device that we used during our research.	36
4.1	Relation between absorbance and wavelenghts of TiO ₂ sample.	39
4.2	Relation between absorption coefficient e and wavelenghts of TiO ₂ sample.	40
4.3	Optical energy band gap of TiO ₂ sample.	40
4.4	Relation between refractive Index and wavelenghts of TiO ₂ sample.	41
4.5	Relation between optical conductivity and wavelenghts of TiO ₂ sample.	41
4.6	Relation between electrical conductivity and wavelenghts of TiO ₂ sample.	42
4.7	SEM image of TiO ₂ .	42
4.8	Histogram SEM image of TiO ₂ .	43
4.9	XRD spectrum of Nano TiO ₂ sample.	44

4.10	FTIR spectrum of TiO₂ sample.	45
4.11	Absorption curves of blood samples that effects by TiO₂ with different concentration (0.1, 0.2, 0.3, 0.4, 0.5, 0.6, 0.7 and 0.8) ppm at First week.	46
4.12	Rated of statically absorption curves riding of blood sample by different concentration of TiO₂ at First week.	47
4.13	Absorption curves of blood samples that effects by TiO₂ with different concentration (0.1, 0.2, 0.3, 0.4, 0.5, 0.6, 0.7 and 0.8) ppm at Second week.	47
4.14	Absorption curves of blood samples that effects by TiO₂ with different concentration (0.1, 0.2, 0.3, 0.4, 0.5, 0.6, 0.7 and 0.8) ppm at Second week.	48
4.15	Absorption curves of blood samples that effects by TiO₂ with different concentration (0.1, 0.2, 0.3, 0.4, 0.5, 0.6, 0.7 and 0.8) at 3red week ppm.	49
4.16	Rated of statically absorption curves riding of blood sample by different concentration of TiO₂ at 3red week.	50
4.17	Absorption curves of blood samples that effects by TiO₂ with different concentration (0.1, 0.2, 0.3, 0.4, 0.5, 0.6, 0.7 and 0.8) ppm at Last week.	50
4.18	Rated of statically absorption curves riding of blood sample by different concentration of TiO₂ at Last week.	51
4.19	Effect of 0.1 ppm TiO₂ on the survival of number of viable cells Escherichia coli (CFU/ml) after 4 weeks on the water.	53

4.20	Effect of 0.2 ppm TiO₂ on the survival of number of viable cells Escherichia coli (CFU/ml) after 4 weeks on the water.	53
4.21	Effect of 0.3 ppm TiO₂ on the survival of number of viable cells Escherichia coli (CFU/ml) after 4 weeks on the water.	54
4.22	Effect of 0.4 ppm TiO₂ on the survival of number of viable cells Escherichia coli (CFU/ml) after 4 weeks on the water.	54
4.23	Effect of 0.5 ppm TiO₂ on the survival of number of viable cells Escherichia coli (CFU/ml) after 4 weeks on the water.	55
4.24	Effect of 0.6 ppm TiO₂ on the survival of number of viable cells Escherichia coli (CFU/ml) after 4 weeks on the water.	55
4.25	Effect of 0.7 ppm TiO₂ on the survival of number of viable cells Escherichia coli (CFU/ml) after 4 weeks on the water.	56
4.26	Effect of 0.8 ppm TiO₂ on the survival of number of viable cells Escherichia coli (CFU/ml) after 4 weeks on the water.	56
4.27	Effect of TiO₂ on the survival of number of viable cells Escherichia coli (CFU/ml) at first week.	57
4.28	Effect of TiO₂ on the survival of number of viable cells Escherichia coli (CFU/ml) at second week.	58
4.29	Effect of TiO₂ on the survival of number of viable cells Escherichia coli (CFU/ml) at thread week.	58

4.30	Effect of TiO₂ on the survival of number of viable cells Escherichia coli (CFU/ml) at last week.	59
4.31	Effect of TiO₂ on the survival of number of viable cells Escherichia coli (CFU/ml) after 4 weeks.	59
4.32	Effect of TiO₂ on the survival pH meter of viable cells Escherichia coli (CFU/ml) at first week.	60
4.33	Effect of TiO₂ on the survival pH meter of viable cells Escherichia coli (CFU/ml) at second week.	61
4.34	Effect of TiO₂ on the survival pH meter of viable cells Escherichia coli (CFU/ml) at thread week.	61
4.35	Effect of TiO₂ on the survival pH meter of viable cells Escherichia coli (CFU/ml) at first week.	62

Chapter one

Introduction

1.1 Nano Science and Biology

The discovery of quantum physics opens a new horizon in physics and modern technology. Quantum mechanics is the branch of physics that describes the nature of individual atoms and elementary particles. [1, 2, 3]. Mechanics can also describe the behavior of these atoms when they combined together to form a bulk matter [4]. From the pure quantum mechanical view point the behavior of isolated atom is different from its behavior when it is surrounded by other atoms to form a bulk matter. The magnetic, electric field and overlap of energy levels affect severely the structure, nature and behavior of this atom [4, 5]. The number of surrounding atoms also affects the physical property of the atom. This means that the size of the physical system affects its physical properties. When the size of the physical system is in the range of inane matter (in $m=10^{-9}m$) up to 300nm, the system is described by quantum laws. However the behavior of the bulk mater with sizes more that few micrometers obeys classical laws [6]. The particles that have sizes in the range (1-300 nm) are called Nano particles. Their behaviors are strongly dependent on their size, structure, geometry and composition. Thus one can change and control to a great extent the physical the desired need properties of Nano material to match [7, 8]. Nano –TiO₂ physical proportions –Effect of TiO₂ on organisms: Nano science it that branch of Science dealing with isolated particles or systems having sizes in the range of Nano meters (1 nm= $10^{-9}m$) in the range of (1- 300 nm). Such that particles are observer to have interesting physical properties, the of the bulk matter. This is due to the fact that the Nano material consists of tiny isolated nano Particles that obeys the lows of Quantum Mechanics In contrast bulk matter obeys classical lows [9]. This interesting Property motivates researchers to try to change Physical Properties of TiO₂ to change Physical Properties of Matter so as to be used in applications in many Areas. One of the Most Interesting Properties is that of Nano TiO₂. Titanium dioxides and some miner are used in many medical and health applications. It can be used in killing organisms, purifying water, or killing cancer cells [10].

1.2 Research Problem

The physical properties of water and blood affect human health. No enough researches were made to apply nano science for changing water and blood properties.

1.3 Aim to the work

The aim of this work is to use Titanium dioxide (TiO_2) for different concentrations to see how blood and water physical properties change.

1.4 Thesis layout

This research include four chapters. Chapter one is the introduction. Chapter two is the theoretical background. Chapter three is the material and method and experimental work. Chapter four is concerned with discussion and conclusion.

Chapter two

Theoretical Background

2.1 Introduction

History of nanotechnology: The history of nanotechnology traces the development of the concepts and experimental work falling under the broad category of nanotechnology. Although nanotechnology is a relatively new, the development of its central concepts happened over a longer period of time. The emergence of nanotechnology in the 1980_s was caused by the convergence of experimental advances such as the invention of the scanning tunneling microscope in 1981 and the discovery of fullerenes in 1985, with the elucidation and popularization of a conceptual framework for the goals of nanotechnology beginning with the 1986 publication of the book *Engines of Creation*. The field was subject to growing public awareness and controversy in the early 2000_s, with prominent debates about both its potential implications as well as the feasibility of the applications envisioned by advocates of molecular nanotechnology, and with governments moving to promote and fund research into nanotechnology. The early 2000_s also saw the beginnings of commercial applications of nanotechnology, although these were limited to bulk applications of nanomaterials rather than the transformative applications envisioned by the field [11].

Early uses of nanomaterial's: The earliest evidence of the use and applications of nanotechnology can be traced back to carbon nanotubes, cementite nanowires found in the microstructure of woods steel manufactured in ancient India from the time period of 600 BC and exported globally [12]. Although nanoparticles are associated with modern science, they were used by artisans as far back as the ninth century in Mesopotamia for creating a glittering effect on the surface of pots [12, 13]. In modern times, pottery from the middle Ages and Renaissance often retains a distinct gold –or copper-colored metallic glitter. This luster is caused by the metallic film that was applied to the transparent surface of a glazing, which contains silver and copper nanoparticles dispersed homogeneously in the glassy matrix of the ceramic glaze. These nanoparticles created by the artisans by adding copper and silver salts and oxides together with vinegar, ochre, and clay on the surface of previously-glazed pottery. The technique originated in the Muslim world. As Muslims were not allowed to use gold in artistic

representations, they sought a way to create a similar effect without using real gold. The solution they found was using Luster [13, 14, and 15]. There's plenty of room at the bottom. The American physicist Richard Feynman lectured, "There's plenty of room at the bottom," at an American Physical Society meeting at Caltech on December 29, 1959, which is often held to have provided inspiration for the field of nanotechnology. Feynman had described a process by which ability to manipulate individual atoms and molecules might be developed, using one set of precise tools to build and operate another proportionally smaller set, so on down to the needed scale. In the course of this, he noted, scaling issues would arise from the changing magnitude of various physical phenomena: gravity would become less important, surface tension and Van der Waals attraction would become more important [15]. After Feynman's death, scholars studying the historical development of nanotechnology have concluded that his actual role in catalyzing nanotechnology research was limited, based on recollections from many of the people active in the nascent field in the 1980s and 1990s. Chris Toomey, a cultural anthropologist at the University of South Carolina, found that the published versions of Feynman's talk had a negligible influence in the twenty years after it was first published, as measured by citations in the scientific literature, and not much more influence in the decade after the Scanning Tunneling Microscope was invented in 1981. Subsequently, interest in "plenty of Room" in the scientific literature greatly increased in the early 1990s. This is probably because the term "nanotechnology" gained serious attention just before that time, following its use by K. Eric Drexler in his 1986 book, *Engines of Creation: The Coming Era of Nanotechnology*, which took the Feynman concept of a billion tiny factories and added the idea that they could make more copies of themselves via computer control by human operator [16, 17]. Published later that year in a mass-circulation science-oriented magazine, *OMNI*. Toomey's analysis also includes nanotechnologists who say that "plenty of Room" did not influence their early work, and in fact most of them had not read it until a later date [18, 19]. These and other developments hint that the retroactive rediscovery of Feynman's "plenty of Room" gave nanotechnology a packaged history that provided an early date of December 1959, plus a connection to the charisma and genius of Richard Feynman's stature as a Nobel laureate

and as an iconic surely helped advocates of nanotechnology and provided a valuable intellectual link to the past. [20]

Nano” – From the Greek word for “dwarf” and means (10⁻⁹,) or one-billionth. Here it refers to one-billionth of a meter, or 1 nanomete (1nm). 1 nanometer is about 3 atoms long. “Nanotechnology” – Building and using materials, devices and machines at the nanometer (atomic/molecular) scale, making use of unique properties that occur for structures at those small dimensions. Most consider nanotechnology to be technology at the sub-micron scale. (1-100’s) of nanometers. **How small is a nanometer?** (And other small sizes) [21]. Ratio of surface area-to-volume of structure increases (most atoms are at or near the surface, which make them more weakly bonded and more reactive) Quantum mechanical effects are important (size of structure is on same scale as the wavelengths of electrons, and quantum confinement occurs resulting in changes in electronic and optical property Much of the motivating force and technology for nanotechnology came from the integrated circuit industry As with the fabrication of integrated circuits (IC’s), nanotechnology is based on building structures and systems at very small sizes Done to enhance performance (like IC’s) and as well as result in new properties and applications Can involve combinations of many types of systems (mechanical, biological, chemical, optical, as well as electronic) [22].

2.2 Titanium dioxide

Titanium dioxide is a metal oxide mineral composed of the elements of titanium and oxygen with the chemical formula TiO₂. Titanium dioxide has three crystalline forms including rutile, anatase and brocite. Usually at low temperatures, titanium dioxide crystallizes as anatase phase. With high temperature, the semi-stable phase of anatase transforms into a stable phase of rutile in one transformation [23]. Titanium dioxide nanoparticles have two very specific and interesting properties that give special applications to this material. These two properties are: the photocatalytic property and the hydrophilic property which rise to the properties of titanium dioxide nanoparticles in their self-healing surfaces, anti-microbial surfaces, water purifiers, and air purifiers. There are several novel methods used for the synthesis of titanium dioxide nanoparticles. The most important of these methods include hydrothermal, mechanical, mechanical

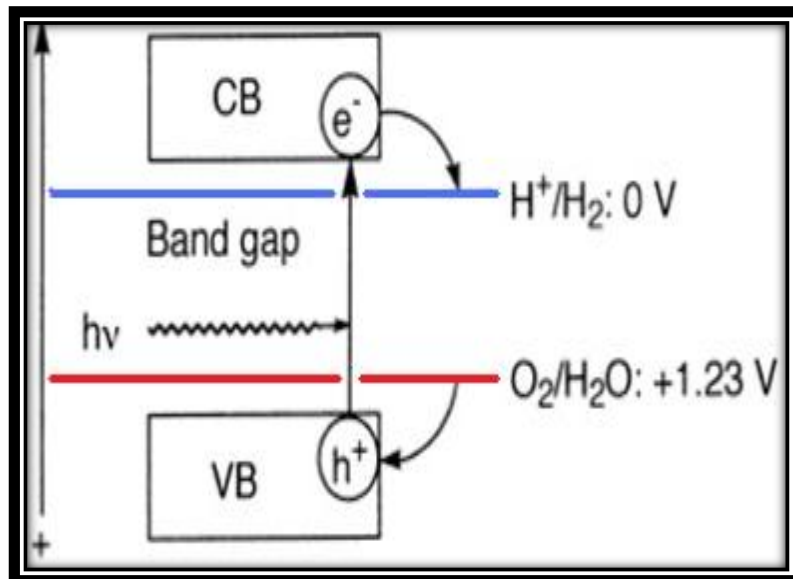
Radiofrequency thermal plasma are chemical vapor condensation and sol-gel. Among the methods mentioned, the sol-gel method has the advantages of fine particle size distribution, chemical composition control and the creation of a thin layer on the surfaces. In 2007, Venkatachalam et al. Produced TiO₂ nanoparticles by sol-gel method. In this work titanium isopropoxide, acetic acid and water with specific molar ratio were used [24, 25]. The results showed that this method is defective for the production of this powder due to its tendency to rapidly agglomerate against crystallization. However, it was found that high calcined temperature caused the formation of TiO₂ crystalline particles. Researchers are also worked on TiO₂ microstructural changes using ultrasound on the sol-gel technique. [26]. the results showed that the crystalline powder is fully formed in this process and the ultrasound waves accelerate the crystallization process. This saves time and energy. Fallah et al. (2014) studied the effect of curing temperature on the electrical and optical properties of TiO₂ nanoparticles in the presence of Niobium based sol-gel method. The results showed that the two-phase atmosphere in the atmosphere greatly increased the film's media attention. Also in this case the electrical resistance is also significantly reduced. Studies were also performed on the microstructural properties of TiO₂ obtained by sol-gel method in the presence of mercury ion and the effect of annealing temperature. The presence of mercury ions will lead to better nanostructure and growth. In addition, in the presence of mercury ions, the reflectance power of the film increases sharply. In 2015 Agartan et al. studied the initial water content and calcination temperature based on sol-gel method on the photocatalytic properties of solid TiO₂ nanoparticles. It has been found that increasing the initial water makes the powders more crystalline and easier to crystallize without sedimentation. The results showed that despite the low temperature of synthesis, the TiO₂ nanopowder was formed with anatase phase in spite of the low temperature of synthesis [27]. Also, with the increase in acetic acid, the faster anatase phase is formed and the formation energy is reduced. In view of the above, it is difficult to obtain TiO₂ nanoparticles that contain both anatase and rutile phases, as well as particles lacking agglomeration and have a good dispersion. Therefore, the aim of this study was to synthesize TiO₂ nanoparticles at rutile phases by sol-gel method and study The Optical and crystalline properties. Various

nanoparticles can be obtained with appropriate dispersion phases and with fine aggregation [28, 29].

2.3 TiO₂ as Photo Catalysis

Various parameters and quantum yields of the photo catalytic hydrogenation reactions of CH₃CCH with H₂O over Rutile-Type (top) and Anatase-Type (bottom) TiO₂ at 300 K affect TiO₂ reactions. Quantum yield = (number of photo formed products) / (number of incident photons). Photo catalytic properties of TiO_{2-x}N_x samples (solid circles) compared with TiO₂ samples (open squares) shows the importance of catalysis. Decomposition of methylene blue as a function of the cutoff wavelength of the optical high-path filters under fluorescent light between 350 and 520 nm, compared with the results under BL illumination with the integrated in the UV range is very important for understanding TiO₂ reactions. The main function of the TiO₂ photo catalyst is to adsorb organic and inorganic contaminants. Under the influence of the UV lamp they later get decomposed into CO₂ and H₂O [30]. Principle of operation and energy level scheme of the dye-sensitized nanocrystalline solar cells. S: Photoexcitation of the sensitizer the dye molecule is regenerated by the redox system, which itself is regenerated at the counter-electrode by electrons passed through the load [31].

Photocatalytic Water Splitting:



Figuer (2.1): The principle of water splitting using a semiconductor photocatalyst.

The bottom level of the conduction band has to be more negative than the reduction potential of H^+ / H_2 (0 V vs. NHE). The top level of the valence band has to be more positive than the oxidation potential of O_2 / H_2O (1.23 V). Strategy of the development of photocatalysts with a visible light response.

- To form a donor level above a valence band by doping some element into conventional photocatalysts with wide band gaps such as TiO_2 .
- To create a new valence band employing some element.
- To control the band structure by making a solid solution. [32].

Electrochromic Devices: Principle of signal amplification by a TiO_2 nanocrystalline film.

The device could be switched back and forth between the colorless and colored states within 1 s [10]. First reduction potential: 0.2 – 0.6 V Second reduction potential: 0.2 – 0.4 V.

The principle of water splitting using a semiconductor photocatalyst: The bottom level of the conduction band has to be more negative than the reduction potential of H^+ / H_2 (0 V vs. NHE). The top level of the valence band has to be more positive than the oxidation potential of O_2 / H_2O (1.23 V). Strategy of the development of photocatalysts with a 2-4-2-2-7-13 visible light response:

- To form a donor level above a valence band by doping some element into conventional photocatalysts with wide band gaps such as TiO_2 .
- To create a new valence band employing some element.
- To control the band structure by making a solid solution [33].

Polyfunctional Adsorbent Crystal Structure: New nanohybrid compound combining the redox functionality of hydrazine, the ionexchange properties of layered titanate, the large surface area of quasi-two-dimensional crystal structures, surface Brønsted acidity, and the occurrence of surface titanyl bond. It possesses a high uptake capacity of ~50 elements of the periodic table. Projections onto (right) (001) and (left) (100). Edge-faced stacking of corner-sharing TiO_6 octahedra (Yellow) results in the formation of interlayer “pseudochannels” directed along the c axis. These pseudochannels are half-occupied by hydrazinium ions (blue spheres depict the front row and grayish spheres the back row)

tailored in such a way that NN bonds are directed along the pseudochannels. The relative sizes of the shown structural units are consistent with their actual size ratios [34].

Adsorbent Functionalities: LHT-9 is an effective reducing agent that has the redox properties of hydrazine superimposed onto the adsorption properties of the nanocrystalline titanate matrix, resulting in the phenomenon of reductive adsorption. The irreversibility of the majority of reduction reactions under the given redox conditions, LHT-9 can be used for cumulative extraction of reducible elements from their solutions.

Redox Properties [35]. Ion Exchange Properties: LHT-9 exhibits high rates of ion-exchange and protonation reactions. The majority of exchange products however, were found to contain hydrazinium [36].

Surface Acidity Properties: Brønsted acidity is likely caused by protonation of bridging Ti-O-Ti oxygen atoms located at loose corners of TiO₆ octahedra exposed at the surfaces of the titanate layers [37].

Summary: TiO₂ has various functionalities not only to be used for white source of paints and cosmetics expected to reflect UV light, they also have light sensitivity and modified it has adsorption capacity. TiO₂ nanomaterials have significant differences by nanoparticle size and geometry. It is necessary to select suitable reaction condition to synthesize objective particle shape materials. Photocatalytic and photovoltaic tec. are begun to use various fields, for example, solar panel, pollutant decomposition, superhydrophilic materials and water splitting, etc. Although TiO₂ is NOT used industrially since less effectivity, today I introduced, some solubility to improve light effectivity are studying with all one's heart!

2.4 Synthetic Methods

There are many methods for synthetic TiO₂ like Sol-Gel Method, Micelle and Inverse Micelle Method, Sol Method, Hydrothermal Method, Solvothermal Method. In Sol-Gel Method: process one normally proceeds via an acid-catalyzed hydrolysis step of titanium (IV) lakeside followed by condensation. The development of Ti-O-Ti chains is favored with low content of water, low hydrolysis rates, and excess titanium lakeside in the reaction mixture. 3-dimensional polymeric skeletons with close packing result from the development of Ti-O-Ti chains. Amines are used as the shape controllers of the TiO₂ nanomaterial's act as Surfactants. Amines include triethanolamine (TEOA), diethylethlenetriamine, ethylenediamine, trimethylenediamine and triethylenetetramine. The morphology of the TiO₂ nanoparticles changes from cuboidal to Ellipsoidal at pH above 11. The shape control is attributed to the tuning of the growth rate of the different crystal planes of TiO₂ nanoparticles by the specific adsorption of shape controllers to these planes under different pH conditions [38].

Sol-Gel Method 1: Amines are used as the shape controllers of the TiO₂ nanomaterials act as surfactants. Amines include triethanolamine (TEOA), diethylethlenetriamine, ethylenediamine,

trimethylenediamine and triethylenetetramine. The morphology of the TiO₂ nanoparticles changes from cuboidal to ellipsoidal at pH above 11. The shape control is attributed to the tuning of the growth rate of the different crystal planes of TiO₂ nanoparticles by the specific adsorption of shape controllers to these planes under different pH conditions [39]. Sol Method2: The sol method is the nonhydrolytic sol-gel processes and usually involves the reaction of titanium chloride with a variety of different oxygen donor molecules, e.g., metal alkoxide or organic ether. To control particle size: Increased nucleophilicity (ore size) of the halide resulted in smaller anatase Nano crystals, e.g., average sizes ranged from 9.2 nm for Tif₄ to 3.8 nm for Tif₄. Reaction in pure trioctylphosphine oxide (TOPO) was slower and resulted in smaller particles, while reactions without TOPO were much quicker and yielded mixtures of brookite, rutile, and anatase with average particle sizes greater than 10 nm. The most stable formThe solvothermal method is almost identical to the hydrothermal method except that the solvent used here is nonaqueous. The temperature can be elevated much higher than that in hydrothermal method. The solvothermal method normally has better control than hydrothermal method of the size and shape distributions and the crystallinity of the TiO₂ nanoparticles [40].

2.5 Optical Parapets

2.6 2.5.1 Absorption

The intensity of the net absorbed radiation is dependent on the character of the medium as well as the path length. The intensity of transmitted or non-absorbed radiation continuously decreases with distance x that the light traverses according to the relation [3].

$$I_T = I_0 e^{-\beta x} \dots\dots\dots (2.1)$$

Where I_T, I₀, β stands for the intensity at x, intial intensity and absorption coefficient respectively. Where is the intensity of the non-reflected incident radiation and β the absorption Coefficient (in mm-1), is characteristic of the particular material; furthermore, varies with wavelength of the incident radiation. The distance parameter x is measured from the incident surface into the material. Materials that have large values are considered highly absorptive [4].

2.5.2 Transmission

The phenomena of absorption, reflection, and transmission may be applied to the passage of light through a transparent solid. For an incident beam of intensity I₀ that impinges on the front surface of a specimen of thickness l and absorption coefficient, the transmitted intensity at the back face I_T is

$$I_T = I_0 (1 - R)^2 e^{-\beta l} \dots\dots\dots (2.2)$$

Where R is the reflectance; for this expression, it is assumed that the same medium exists outside both front and back faces. The derivation of Equation (2.2) is left as a homework problem. Thus, the fraction of incident light that is transmitted through a transparent material depends on the losses that are incurred by absorption and reflection. Again, the sum of the reflectivity R, absorptivity A, and transmissivity T, is unity according to Equation (2). Also, each of the variables R, A, and T depends on light wavelength. This is demonstrated the transmission [3.4 and5].

2.5.3 Absorption coefficients

Much of the information about the properties of materials is obtained when they interact with electromagnetic radiation. When a beam of light (photons) is incident on a material, the intensity is expressed by the Lambert-Beer-Bouguer law [6].

$$I = I_0 \exp(-\alpha d) \dots\dots\dots (2.3)$$

If this condition for absorption is met, it appears that the optical intensity of the light wave, (I), is exponentially reduced while traveling through the film. If the power that is coupled into the film is denoted by I₀, gives the transmitted intensity that leaves the film of thickness d. (α) is called “absorption coefficient” [6]. From (1) it follows that

$$\alpha = -\frac{1}{d} \text{Lin}\left(\frac{I}{I_0}\right) \dots\dots\dots (2.4)$$

It is clear that α must be a strong function of the energy hv of the photons. For hv < E_g (direct), no electron hole pairs can be created, the material is transparent and α is small. For hv ≥ E_g (direct), absorption should be strong. All mechanisms other than the fundamental absorption may add complications (e.g. "sub band gap absorption" through excitons), but usually are not very pronounced [6]. Optical transmission measurements were carried out to determine the film thickness, the wavelength dependence of the refractive index and optical absorption coefficient. The optical constants were determined from the optical transmission measurements using the method described by Swanepoel. The transparent substrate has a thickness several orders of magnitude larger than (d) and has index of refraction (n) and absorption coefficient (α = 0). The index of refraction for air is taken to be n₀ = 1. In the transparent region (α = 0) the transmission is determined by n and s through multiple reflections. In the region of weak absorption α is small and the transmission begins to decrease. In the medium absorption region α is large and the transmission decreases mainly due to the effect of α. In the region of strong absorption

the transmission decreases drastically due almost exclusively to the influence of α . If the thickness d is uniform, interference effects give rise to the spectrum [5, 6].

2.5.5 Reflection

When light radiation passes from one medium into another having a different index of refraction, some of the light is scattered at the interface between the two media even if both are transparent. The reflectivity R represents the fraction of the incident light that is reflected at the interface, or

$$R = \frac{I_R}{I_0} \dots\dots\dots (2.5)$$

Where I_0 and I_R are the intensities of the incident and reflected beams, respectively. If the light is normal (or perpendicular) to the interface, then

$$R = \left(\frac{n_2 - n_1}{n_2 + n_1}\right)^2 \dots\dots\dots (2.6)$$

Where n_1 and n_2 are the indices of refraction of the two media. If the incident light is not normal to the interface, R will depend on the angle of incidence. When light is transmitted from a vacuum or air into a solid s , then

$$R = \left(\frac{n_s - 1}{n_s + 1}\right)^2 \dots\dots\dots (2.7)$$

Because the index of refraction of air is very nearly unity. Thus, the higher the index of refraction of the solid, the greater the reflectivity [6].

2.5.6 Refractive index

Light that is transmitted into the interior of transparent materials experiences a decrease in velocity, and, as a result, is bent at the interface; this phenomenon is termed refraction. The index of refraction n of a material is defined as the ratio of the velocity in a vacuum c to the velocity in the medium or

$$n = \frac{c}{v} \dots\dots\dots (2.8)$$

The magnitude of n (or the degree of bending) will depend on the wavelength of the light. This effect is graphically demonstrated by the familiar dispersion or separation of

a beam of white light into its component colors by a glass prism [9]. Each color is deflected by a different amount as it passes into and out of the glass, which results in the separation of the colors. Not only does the index of refraction affect the optical path of light, but also, as explained shortly, it influences the fraction of incident light that is reflected at the surface [9]. Just as Equation (2.8) defines the magnitude of c , an equivalent expression gives the velocity of light in a medium as

$$v = \frac{1}{\sqrt{\epsilon\mu}} \dots\dots\dots (2.9)$$

Where ϵ and μ are, respectively, the permittivity and permeability of the particular substance [8]. From Equation (2.8), we have

$$n = \frac{c}{v} = \frac{\sqrt{\epsilon_0\mu_0}}{\sqrt{\epsilon\mu}} = \sqrt{\epsilon_r \mu_r} \dots\dots\dots (2.10)$$

Where ϵ_r and μ_r are the dielectric constant and the relative magnetic permeability, respectively. Because most substances are only slightly magnetic, and

$$n \cong \sqrt{\epsilon_r} \dots\dots\dots (2.11)$$

Thus, for transparent materials, there is a relation between the index of refraction and the dielectric constant [8].

2.5.7Determination of Band Gaps

The fundamental absorption is related to band-to-band or to exaction transition, which are subjected to certain selection rules [17]. The transitions are classified into several types, according to the band structure of a material. The relation between absorption coefficient and optic band gap for direct transition ($k=0$) is given by Tauc equation.

$$\sqrt{\alpha h\nu} = B(h\nu - E_g^{opt}) \dots\dots\dots (2.12)$$

And for indirect transition ($k \neq 0$) the relation becomes

$$\alpha(h\omega) \propto \frac{(\hbar\omega - E_{gap})^2}{\hbar\omega} \dots\dots\dots (2.13)$$

From the $\alpha h\nu$ versus $h\nu$ one obtains E_g and B parameters. B is also a useful diagnostic of the material since it is inversely proportional to the extent of the tail state (ΔE) at conduction and valance band edges [8 and9].

2.6 Human Blood

Blood is a connective tissue performs two major functions transport materials through the body to play as mediators to defense of the body against infections and other foreign materials .It functions related to maintaining and balancing homeostasis of the body pumped by heart and carried by blood vessels throughout the body. Primarily, to transport oxygen, nutrients, chemical and cell wastes to certain targeted area .Blood makes up about 7% of body depending on his or her size. Colour of the blood does vary for example, arterial blood is bright red because it contains high levels of oxygen but venous blood (most is deoxygenated) has a darker, dull red colour. The normal pH range of blood is 7.35 to 7.45, which is slightly alkaline. Blood is about three to five times thicker than water. Viscosity is increased by the presence of blood cells and the plasma proteins, and this thickness contributes to normal blood pressure (Nursakina. 2015). It composed of plasma and seven types of cells, red blood cells (RBC) or erythrocytes, platelets or thrombocytes .And five kinds of white blood cells (WBC) or leukocyte .All the various types of blood cells are produced in the bone marrow .Arise from a single type of cell called a hematopoietic stem cell [22].

2.6.1 White Blood Cell count (WBC)

Is the number of white blood cells in a volume of blood, normal range varies slightly between laboratories but generally between 3,400 and 10,800 calls per cubic millimeter (mm).This can also be referred to as the leukocyte count and can be expressed in international units as 4.3 to 10.8×10^9 cells per litter .White blood cells are comprised of several different types that are differentiated based on their size and shape.The Complete Blood Count (CBC)provide account of white blood cells and also an automated differential count that determines the percentage of the five types of mature white blood cells present in the human body .Which were divided as follow, and their man functions: Neutrophils) NEUT) :(granulocytes) arechemotaxis, phagocytosis and killing of phagocytized bacteria .The normal range between 50 – 70% Lymphocytes(LYM): are involved in immune responses and production of haemopoietic growth factors .The

normal range is 25 – 35% Basophiles (granulocytes) they were Mediate immediate-type hypersensitivity) IgE-coated basophils react with specific antigen and release histamine and leukotriene's), modulate inflammatory responses by releasing heparin and proteases . The normal range 0.4 – 1 % Eosinophil's (: granulocytes) beside all neutrophil function listed above they are effector cells for anti-body-dependent damage to metazoan parasites, regulate immediate-type hypersensitivity reactions (inactivate histamine and leukotriene's released by basophils and mast cells) .The normal range is (1–3).% Monocytes:4–6(%Macrophages)are chemo taxis, phagocytosis, killing of some microorganisms' antigen presentation, release of IL-1 and TNF which stimulate bone marrow stromal cells to produce GM-CSF, M-CSF and IL-6[23]. The last three types are counted together and they called mixed (MXD).The white blood cell count helps provide information about various illnesses and also help monitor the patient's recovery once treatment is started [23].

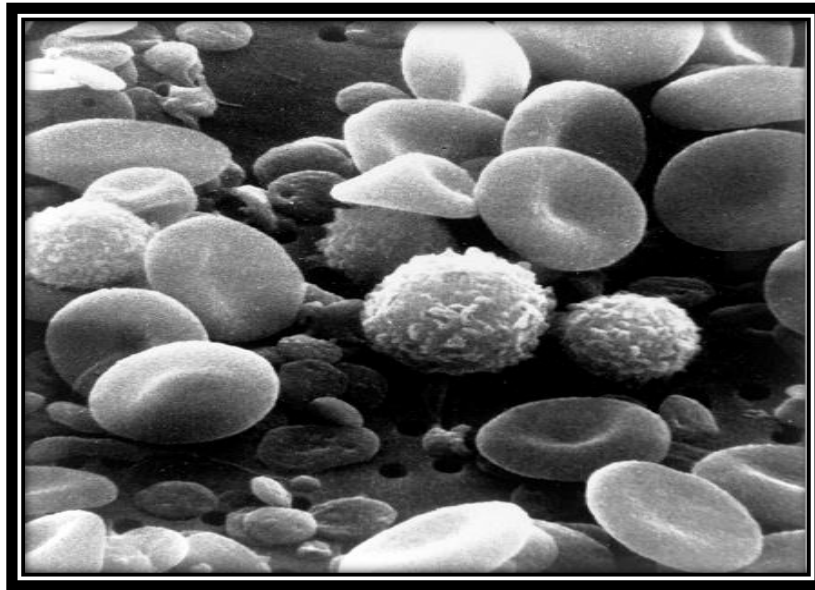


Fig (2.2) White Blood Cell count (WBC) [23].

2.6.2 Red Blood Cell count(RBC)

Are the most common cell type in blood and people have millions of them in their blood circulation .They are smaller than white blood cells, but larger than platelets .The production of red blood cells is referred to as erythropoiesis .Mature red blood cells

develop from haemocytoblasts .This development takes about 7 days and involves three to four mitotic cell divisions, so that each stem cell gives rise to 8 or 16 cells. In health, erythropoiesis is regulated so that the number of circulating erythrocytes is maintained within a narrow range .Normally, a little less than 1 %of the body’s total red blood cells are produced per day and these replace an equivalent number that have reached the end of their life span .However that still represents a huge 200,000,000,000 cells.Erythropoiesis is stimulated by hypoxia (lack of oxygen) .However, oxygen lack does not act directly on the haemopoietic tissues but instead stimulates the production of a hormone”erythropoietin” .This hormone then stimulates haemopoietic tissues to produce red cells .Normal range varies with altitude :Male :4.7 to 6.1 million cells/ μ l (per misrelate of blood) .Female: 4.2 to 5.4 million cells/ μ l. Children: 4.6 to 4.8 million cells/ μ l [22, 23].



Fig (2.3) Red Blood Cell count(RBC) [23].

2.6.3Platelets (PLT)

Platelets are produced in bone marrow by process known as thrombopoiesis .They are formed in the cytoplasm of a very large cell, the megakaryocyte .Megakaryocyte matures in about 10 days, from a large stem cell, megakaryoblast. It is likely that there are

thrombopoietic feedback mechanisms as the platelet count remains fairly constant in health and platelet production is reduced following an infusion of platelets and increased following removal of platelets .However, these feedback mechanisms have not been discovered yet .At any one time, about two-thirds of the body's platelets are circulating in the blood and one-third are pooled in the spleen .There is constant exchange between the two populations .The life span of platelets is between 8 to 12 days .They are destroyed by macrophages, mainly in the spleen and also in liver.The number of platelets in a specified volume of blood and the platelets are not complete cells, but actually fragments of cytoplasm (part of a cell without its nucleus, or the body of a cell.) The normal range can be expressed in a number of ways, but they all mean the same. 150,000 – 350,000 / μ l (platelets per micro Litre) [24].

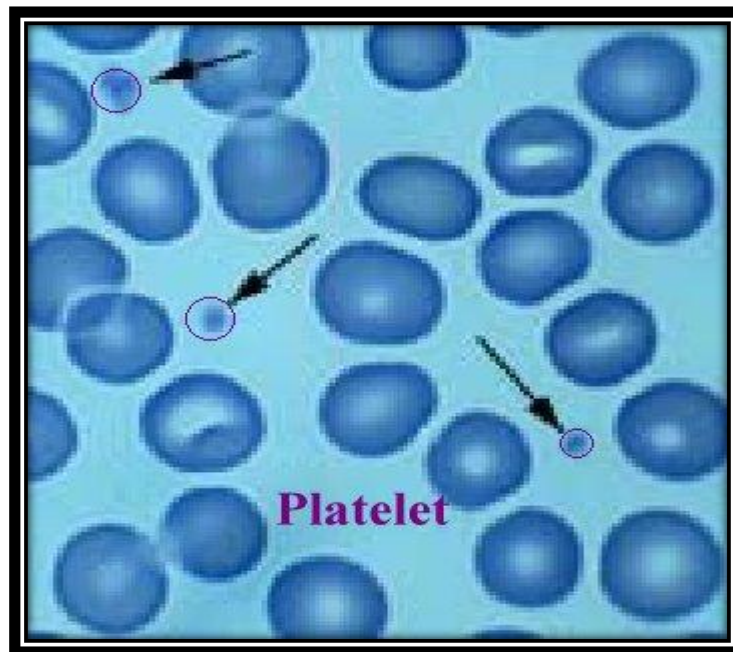


Fig (2.4) Platelets (PLT) [24].

2.6.4 Hemoglobin (HGB)

Oxygen and som carbon dioxide transport depends almost totally on the presence of the red respiratory pigment haemoglobin in the erythrocyest. Haemoglobin increases the ability of the blood to carry oxygen by 60-flod.This vital funcnion makes haemoglobin

on. This is the amount of hemoglobin in a volume of blood .Hemoglobin is the protein molecule within red blood cells that carries oxygen and gives blood its red color .Normal range of hemoglobin is different between the sexes : Male: 8.1 to 11.2 m/mol/L(13 to 18mg/dl) . Female :7.4 to 9.9 m/mol/L) 12 to 16 mg/dl). Child :–7.1 to 8.4 m/mol/L) 11.5 to 13.5 mg/dl) .Newborns :–10.5 to 13.7 m/mol/L) 17 to 22 mg/dl) [22, 23].

2.6.5Hematocrit (HCT)

This is the ratio of the volume of red cells to volume of whole blood .Normal range for hematocrit is different between the sexes and is approximately 45 %to 52 %for men and 37 %to 48 %for women .This is usually measured by spinning down a sample of blood in a test tube, which causes the redblood cells to pack at the bottom of the tube [22].

2.6.6Mean Corpuscular Volume (MCV)

It’s the average volume of a red blood cell.This is calculated value derived from the hematocrit and red cells count .Normal range may fall between 80 to 100 fl) femtoliters [22].

2.6.7Mean Corpuscular Hemoglobin (MCH)

Is the average amount of hemoglobin in the average red cell.This is a calculated value derived from the measurement of hemoglobin and red cells count .Normal range is 27 to 23 pg) pico g) [23].

2.6.8Mean Corpuscular Hemoglobin Concentration (MCHC)

Is the average concentration of hemoglobin in a given volume of red cells.This is calculated value derived from the hemoglobin measurement and the hematocrit .Normal range is 32 %to 36.% [23].

2.6.9Optical properties of blood

The optical properties of human blood measured at different wavelengths (in vitro, ex vivo and in vivo) [22].

Table (2.1) Optical properties of human blood [24].

Wavelength (nm)	$\mu\text{a cm}^{-1}$	$\mu\text{s cm}^{-1}$	G
517	354	468	0.995

585	191	467	0.995
590	69	466	0.995
595	43	465	0.995
600	25	464	0.995

Where: μ_a =the absorption coefficient μ_s = the scattering coefficient g =the scattering anisotropy parameter [24].

2.7 Wastewater Treatment

The significance of the wastewater treatment, management and its disposal gradually increases in the modern times and it becomes a major concern for public health scientific interest. All existing protocols for treatment of wastewater are categorized as physical, chemical and biological processes [41]. The sequential and concurrent use of those processes combinedly tends to create a greater efficient method in removing the pollutant aspects in liquid residues. Restrictions in terms of execution, efficiency, and price are a factor, however, biological processes, as an example, have been extensively used and show potential towards dairy and agricultural wastewater treatment [42]. The chemical process deals with the photocatalysts like TiO_2 , ZnO etc. mediated degradation of the industrial waste waters [43]. These processes have limitations which can potentially affect degradation efficiency through control pH range, rapid organic-load variations, and also the effluent's physicochemical behavior [44]. The use of a heterogeneous photocatalyst is a conventional method for water purification which includes reduction and oxidation reactions from adsorbed wastewater, oxygen molecules and hydroxyl anions, or other organic molecules [45,48]. Uses of semiconductors like TiO_2 , ZnO etc. in photocatalysis employ semiconductors in suspension. However, this method could be a more expensive when it is scaled-up because particle-recovery of the photocatalyst particles is a difficult task and leads to an amplification in process costs. A feasible alternative is the preparation of photocatalyst layers in different substances or uses the catalytic support without hampering the photocatalyst activity [49]. Many efforts have been made in which few studies have demonstrated continuous flow reactors with fixed-bed photocatalyst [50]. Integral to this study was an assessment of the efficiency of heterogeneous photocatalyst processes for dairy and agricultural wastewater treatment

with immobilized TiO_2 and ZnO to reduce organic pollutant load [51]. The immobilization was carried out by the application of a coating containing the Catalysts [52]/photocatalyst [33] or by using the porous carbon or silica as a supporter for the catalysts to prevent agglomeration of catalyst during catalytic/photocatalytic reactions in solution. Moreover, solar emission was used as UV source [53, 55]. Recent review is focused on the most important photocatalysts titanium dioxide and zinc oxide and their photocatalytic activity towards wastewater treatment. Recently, Xiaobo and Samue[I] reviewed the broad applications of titanium dioxide as a photocatalysts [56]. These applications were comprised of photodecomposition of various industrial pollutants, killing tumor cell and killing bacteria in cancer treatments [57]. Semiconductor catalysts TiO_2 and ZnO have been widely used to mineralize harmful organic pollutants in wastewater into less damaging inorganic nontoxic compounds like CO_2 , HCl and water [58]. Several studies have been carried out for decolorization of industrial wastewater by using photocatalysis and bacteria treatment [59, 61]. The elimination of color from wastewaters is more necessary than the removal of other colorless organic compounds¹⁹. Because of aesthetic and environmental concerns the decolorization of effluent from textile dyeing and finishing industry has given most importance [62, 23]. TiO_2/ZnO photocatalysis, in the presence of UV irradiation can disintegrate the pollutant dyes into non-toxic simple compounds like CO_2 , HCl and water [64]. Nanosized TiO_2 and ZnO photocatalysts in the form of nanorods, nanospheres, thin porous films, nanofibers and nanowires have been utilized in various applications, including photocatalysis because of their high activity, low cost and environmental safety [65, 67]. Interestingly, very high surface to volume ratio of nanostructures make them efficient for photocatalysis and other application. In recent studies [53, 64], authors have reported that zinc oxide and titanium dioxide have excellent photocatalytic properties and both catalysts are designated to be capable substrates for photodegradation of dyes water pollutants as they exhibit the acceptable activity in the range of ultraviolet radiation. Various studies have focused on treatment of industrial wastewater using different treatment methods; however, most of these treatments have intricacy in realistic uses [45, 49, 66, 68, and 69]. In recent year, investigation on different systems have been carried out, such as, advanced oxidation processes (AOP) [70], ozonation [71, 72], sonolysis³³,

gamma-radiolysis [74], electro-coagulation [35, 36], H₂O₂/ UV37, photocatalysis24, photo-Fenton [38], biological and combined anaerobic-photocatalytic treatment [59,61and79]. The aim of the present investigate is to investigate photocatalytic oxidation process for the decomposition wastewater using TiO₂ and ZnO as photocatalysts irradiated with artificial ultraviolet radiations. Photocatalytic oxidation processes [70], which involve the generation of highly reactive hydroxyl radical (HO), have emerged as a promising water and wastewater treatment technology for the degradation or mineralization of a wide range of organic contaminants [70, 80and 91]. The photoactivated reactions are characterized by the free radical mechanism initiated by the interaction of photons of a proper energy level with the catalyst (TiO₂, ZnO semiconductor catalysts) [42, 43]. The efficiency of a photocatalytic system is also affected by the form of TiO₂ and ZnO nanoparticle catalysts used as immobilized on surface or as colloidal suspension [84, 86]. The photocatalysis reaction effective for the degradation of various organic impurities in waste water; however,its practical application as slurry type suspensions is limited due to the difficulty in separating the nanocatalysts particles after the photocatalytic reaction[87-89]. The present review aims to provide a comprehensive analysis on the mechanism of UV-TiO₂ and ZnO photocatalytic oxidation process, photocatalyst material, irradiation sources, effect of pH, temperature, dye concentration, catalyst mass and type of catalysts on photocatalysis and the application towards wastewater treatment [89].

2.8 Literature Review

The effect of radiations a nano particle on loud, water and other vitalities are very important for human health. There are many papers published concerning this issue.For example yellow laer of 589 nm wavelength was ued to irradiate human blood samples with random deseases for different irradiation [90]. The lasr power used is 45 w/cm² with eposuer times 10 minutes up to 60 mintes, where diferent exposure time 10 minutes up to 60 minutes. The result obtatined shows change of light absorption with exposure time. The maximum observed absorption is at 40 minute irradiation time at 340 nmm peak. Blood smear of the samples reveals that there are observable changes in the morphology of the red blood cell at 40 minutes and 60 minutes of irradiatsiti. [90]. Another work was done to study effects of low power violet laser irradiation on red blood cells volume and

erythrocyte sedimentation rate in human blood. Samples rheological factors such as mean red blood cell volume (MCV) and erythrocyte sedimentation rate (ESR) were also studied. Samples were irradiated for 20, 30, 40 or 50 min using a laser of power 10 mW. The measurements were done directly after irradiation by applying westergen method and a computerized hemtoanalyzer. The RBCs volume and ESR were decreased after irradiation for 40min by 0.44% and 6.7% respectively. It is possible to this can be attributed to the fact that reduction red blood cells volume results from increased concentrations of free intracellular Ca^{+2} . The result shows that ESR reduction exposed to low power laser is due to the effect of laser on composition of the plasma that finally affects in ESR of whole blood. [91].

Same researchers studies the effect of laser on erythrocytes sedimentation rate and some hematological parameters. Background: This study was conducted in pursuit of gaining an understand effects of the low level laser irradiation on whole blood is very essential way in revealing the mechanisms of the action of laser radiation on biological tissues. Objective: The purpose of this study is to investigate the in vitro effect of laser radiation on some hematological parameters and erythrocyte sedimentation rate. Subject and Method. Blood samples were obtained from 30 healthy volunteers, each sample was divided into four new samples, one of them was considered as control while the other three were exposed to three different laser doses. The wavelength of 532nm was used for irradiation with 4mm diameter beam spot on blood samples, with power density of $796.17mW/cm^2$. The irradiation times were 1.8, 3.7 and 6.2 second so the different doses of irradiation 1.5, 3 and 5 J/cm^2 , respectively. Results: The erythrocyte sedimentation rate was measured after laser irradiation and compared with un-irradiated control sample. The results of this study showed that erythrocyte sedimentation rate value increased significantly with a dose of $1.5J/cm^2$ but not with the other two doses' values in male persons but not in females. Moreover, the mean cell volume shows significant decrement post irradiation. Conclusion: Laser irradiation induces physical changes in red blood cell membrane permeability and blood viscosity and consequently alters erythrocyte sedimentation rate. [90].

Same reseachers used laser for enhancement of human blood Storage Period by Irradiation of Low Level He-Ne Laser: The aim of the present work is to investigate the effect of the He-Ne laser irradiation on the whole human blood (HB) in order to enhance the conditions of

conservation. The HB was irradiated by He-Ne laser; ($\lambda = 632$ nm, continuous wave, power 30 mW, 2 mm diameter beam spot), electrical properties and complete blood count CBC were measured at three doses (0.0287, 0.0563 and 0.198 J/cm³) to the relevant best exposure dose during storage periods 9, 24, 30, 35 & 50 days. The irradiation process with the selected dose was performed by the exposure of the laser beam on the blood sample flow through narrow tube of cross section area, 0.0831 cm². Blood dielectric parameters, (electric conductivity, dielectric constant, dielectric loss and dipole moment) and CBC, (red blood cell, white blood cell, hematocrit, hemoglobin, mean corpuscular volume, mean corpuscular hemoglobin, and mean cell or corpuscular hemoglobin in concentration) were measured. The obtained results were compared with that of the control and showed that the best irradiation exposure dose suitable for increasing the time of blood storage with minimum changes in properties is 0.198 J/cm³ and storage period of about 50 days. The present study revealed that irradiation by He-Ne laser could be considered a good means to improve the conservation conditions of human blood. [91]. A search was done by some scientists to investigate the in-vitro influence of laser radiation on certain blood indices. Material and Methods. To do this blood samples were obtained from 40 healthy volunteers, and 30 samples were divided into 4 groups, 1 of which was the control and the other 3 of which were exposed to 3 doses of green laser while using ethylene diamine tetra acetic acid (EDTA) as an anticoagulant. Remaining 10 samples were anticoagulated using heparin and grouped into 2 aliquots, 1 of which was the control and the other of which was exposed to a single dose of green laser radiation. The test was achieved at a wavelength of 532 nm and a beam-spot diameter of 4 mm. Irradiation times used were 1.8, 3.7, and 6.2 sec, resulting in irradiation doses of 1.5, 3 and 5 J/cm² respectively. Green laser irradiation promoted significant alterations in the mean corpuscular volume (MCV) of erythrocytes regardless of the type of anticoagulant. It also increased the white blood cell (WBC) count when EDTA was used as the anticoagulant, but not when heparin was used. Conclusion. The type of anticoagulant used may alter the effect of lasers on certain blood parameters. [92]. Q-Switched UV Laser Interactions with the Human Blood in Vitro: A Q-switched UV laser beam emitting wavelength at 355 nm with different energy densities (fluence, J/cm²) was used for shining sixty human blood samples in vitro. Absorption spectra of hemoglobin were

measured for the first time for the samples that exposed to 500 laser pulses in comparison to control samples. It was found that the peak absorbance decreases as the laser fluence increases. This decrease in the peak absorption has been found to be due to the red blood cells deformation and aggregation resulting from the effect of the laser pulses. This phenomenon has been confirmed by examination of the blood cells slides after exposing to the laser radiation. Furthermore, the red blood cells (RBCs) counts were found to be decreased with increasing the laser fluence. The decrease in the RBCs after the irradiation explains the decrease in the hemoglobin absorbance and that represents additional evidence to the structural change according to the optical microscope images. The changes in hemoglobin absorbance are used in a clinically available optical oxymeters. The immediate hematology measurements of the blood samples after the exposure to the laser pulses indicate an increase in the white blood cells (WBCs) of the type basophiles. The measurements were obtained with a significant difference with the level of probability ($p \leq 0.05$) between the laser exposed samples and the control samples. This laser effect is also due to structural changes in the WBCs. The changes in mitochondria resulting in cells division are in a good agreement with many results in the literature for other types of laser irradiation and other types of the WBCs. The proliferation of the basophiles upon laser photolysis plays a vital role in the activation of the immune system and a consequent destruction of pathogens by these cells. [93]. Toxicological effects of titanium dioxide nanoparticles: a review of in vitro mammalian studies, this study work by [90]. The detail of this study are recent rapid advances in nanotechnology raise concerns about development, production route, and diffusion in industrial and consumer products of titanium dioxide nanoparticles (TiO₂-NPs). In fact, compared to recent increase in applications of this nanomaterial, the health effects of human exposure have not been systematically investigated. The aim of this review was to provide a comprehensive overview on the current knowledge regarding the effects of TiO₂-NPs on mammalian cells. Evidence and Information Sources. This review is based on an analysis of the current literature on this topic. State of the Art. Fine TiO₂ particles have been considered as safe and to pose little risk to humans, suggesting that exposure to this material is relatively harmless. However, available data in the literature showed that TiO₂-NPs can cause several adverse effects on mammalian cells such as increase of reactive oxygen

species (ROS) production and cytokines levels, reduction of cell viability and proliferation, induction of apoptosis and genotoxicity. Perspectives and Conclusions: Additional research is needed to obtain up-to-date knowledge on health effects of TiO₂-NPs and to avoid any potential risk correlated to their exposure. Consequently, future studies need to. (1) Use a homogeneous and rigorous exposure classification to clarify how the physicochemical properties of TiO₂-NPs correlate with their toxicological effects. (2) Assess the potential adverse effects of low level exposures to TiO₂-NPs, as most of the information currently available originates from studies in which exposure levels were excessively and unrealistically high. (3) Identify the possible roles of TiO₂-NPs in genotoxicity and carcinogenicity (4) carry out epidemiologic studies of exposed workers to provide an assessment of possible risks correlated to the occupational exposure to TiO₂-NPs [90].

Photocatalytic Water Treatment by Titanium Dioxide: Recent updates: This work done by Manoj A [91]. Lazar, the head line of this work are photocatalytic water treatment using nanocrystalline titanium dioxide (NTO) is a well-known advanced oxidation process (AOP) for environmental remediation. With the in situ generation of electron-hole pairs upon irradiation with light, NTO can mineralize a wide range of organic compounds into harmless end products such as carbon dioxide, water, and inorganic ions. Photocatalytic degradation kinetics of pollutants by NTO is a topic of debate and the mostly reporting Langmuir-Hinshelwood kinetics must accompanied with proper experimental evidences. Different NTO morphologies or surface treatments on NTO can increase the photocatalytic efficiency in degradation reactions. Wisely designed photocatalytic reactors can decrease energy consumption or can avoid post-separation stages in photocatalytic water treatment processes. Doping NTO with metals or non-metals can reduce the band gap of the doped catalyst, enabling light absorption in the visible region. Coupling NTO photocatalysis with other water-treatment technologies can be more beneficial, especially in large-scale treatments. This review describes recent developments in the field of photocatalytic water treatment using NTO [91]. Clayton wright investigate the effects of titanium dioxide nanoparticles on human keratinocytes. Titanium dioxide was observed to cause oxidative stress increase, DNA and cell death beside inflammatory gene upregulation in lung and throat cells. However, the effects on skin cells from long-term topical use of various products

remain largely unknown. This study assessed the effect of specific TiO₂ nanoparticles (H2TiO₇) on a human keratinocyte cell line (HaCaT). A comparative analysis was done using three TiO₂ particles varying in size (Fine, Ultrafine and H2TiO₇) and analyzed their effects on HaCaTs. There is a clear dose-dependent increase in superoxide production, caspase 8 and 9 activity, and apoptosis in HaCaTs after treatment with all three forms of TiO₂. However, there is no consistent effect on cell viability and proliferation with either of these TiO₂ particles. While there is data suggesting UV exposure can enhance the carcinogenic effects of TiO₂. Any significant effect of UV-C exposure accompanied with TiO₂ treatment on HaCaTs was not observed. Furthermore, TiO₂-treated cells showed minimal effects on VEGF upregulation and Wnt signaling pathway thereby showing no potential effect on angiogenesis and malignant transformation. Overall, we report here an increase in apoptosis, which may be caspase 8/Fas-dependent, and that the H2TiO₇ nanoparticles, despite their smaller particle size, had no significant enhanced effect on HaCaT cells as compared to Fine and Ultrafine forms of TiO₂. The conclusion was F-TiO₂, UF-TiO₂ and H2TiO₇ particles induce apoptosis in keratinocytes through caspase 8 and the Fas/FADD pathway. There is a dose-dependent increase in superoxide accumulation and caspase 8 and 9 activity; which are followed by a similar trend in apoptosis. However there was no significant difference in the effects of H2TiO₇ nanoparticles as compared to F-TiO₂ and UF-TiO₂. We also report that the various TiO₂ particles had no consistent effects on cell proliferation, viability and angiogenic/migration/invasion potential in HaCaT keratinocytes and two different lung cell types (Beas-2B and CRL-1490). The increased carcinogenic potential of H2TiO₇ due to its increased surface area and smaller particle size, does not translate into more deleterious effects in skin and lung cells, as compared to the other forms of TiO₂. While this study does not focus on the long-term effects that exposure to TiO₂ may have on skin cells; the inconsistent and inconclusive results here corroborate previously published data on the effect of TiO₂ on skin cells. This data reaffirms the accepted conclusion that the effect of TiO₂ is dependent on the integrity of the epidermal skin layer (more effective on damaged tissue), and the genetic characteristics of the skin layer being exposed to the nanoparticles. Further analysis using long-term exposure studies is definitely needed to determine the cytotoxic or malignant potential of TiO₂ nanoparticles on human skin cells.

This analysis will allow us to make conclusive determinations on what effect, if any, chronic exposure to TiO_2 is having on the human population [92]. Karishma. Of nanotechnology in wastewater applications treatment. Nanoparticles have a great potential to be used in waste water treatment. For unique characteristics of it having high surface area that can be used efficiently for removing toxic metal ions, microbes, inorganic and organic solutes from water. Nanotechnology has led to various efficient ways for treatment of waste water in a more precise and accurate way on both small and large scale. Although nanotechnology enabled water/wastewater treatment processes have shown great promise in laboratory studies, their readiness for commercialization varies widely. Some are already on the market, while others require significant research before they can be considered for full scale applications. Their future development and commercialization face a variety of challenges including technical hurdles, cost-effectiveness, and potential environmental and human risk. There are two major research needs for applications of nanotechnology in water/wastewater treatment. First, the performance of various nanotechnologies in treating real natural and waste waters needs to be tested. Future studies need to be done under more realistic conditions to assess the applicability and efficiency of different nanotechnologies as well as to validate nanomaterial enabled sensing technologies. Secondly, the long-term efficiency of these nanotechnologies is largely unknown as most lab studies were conducted for relatively short period of time. Research addressing the long term performance of water and wastewater treatment nanotechnologies is in great need [93]. Javad sharifi. Rad work is concerned with In-vivo titanium dioxide (TiO_2) nanoparticles effects on chromosomal abnormalities and lactate dehydrogenase activity. For this purpose nano anatase of titanium dioxide in four dosages of 10, 50, 100, 500, 800mg/Kg BW during intraperitoneal injection of male mice Balb/C were treated. After 24 hours, micronucleus test was carried out on the samples of bone marrow for determination of the level of lactate dehydrogenase (LDH) level test performed on the samples of peripheral blood. Result showed that nano anatase of titanium dioxide in low dosage of 10, 50, 100mg/Kg BW, had no toxicity effects on bone marrow. However high doses of 500, 800mg/Kg BW caused induced toxicity effect with increase micronucleus. The dosage of 10mg/Kg BW of nanoparticles showed LDH enzyme is blocked and a reduced in LDH level. Titanium

dioxide has capacity to oxidize the DNA strands of chromosomes on the A-T, G-C base of nucleotides by direct action on three hydrogen bonds of purine moiety and two hydrogen bonds of pyrimidine moiety. So the increasing concentration of TN shows the increasing value of MNPCE. The same event happens in LDE enzyme activity on nanoparticles of titanium dioxide. Since enzyme is macromolecular protein entity made by the genomics of chromosomes of nucleotides which get oxidized by TiO_2 . The base pair of nucleotide of both MNPCE and LDE gets oxidized by its transition metal property [94].

Chapter Three

Experimental work

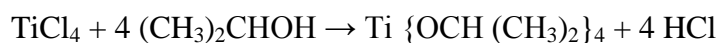
3.1 Introduction

This chapter determines the materials and method used to underpin the experimental of study, the main content include information about: samples, Materials, devices used, and methods.

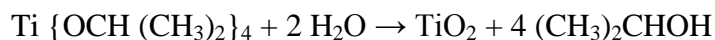
3.2 Material

3.2.1 Titanium Isopropoxide

Titanium isopropoxide, also commonly referred to as titanium tetraisopropoxide or TTIP, is a chemical compound with the formula $\text{Ti} [\text{OCH} (\text{CH}_3)_2]_4$. This alkoxide of titanium (IV) is used in organic synthesis and materials science. It is a diamagnetic tetrahedral molecule. Titanium isopropoxide is a component of the Sharpless epoxidation, a Nobel-Prize-winning method for the synthesis of chiral epoxies [1, 2]. The structures of the titanium alkoxides are often complex. Crystalline titanium meth oxide is turmeric with the molecular formula $\text{Ti}_4 (\text{OCH}_3)_{16}$ [3]. Alkoxides derived from bulkier alcohols such as isopropanol aggregate less. Titanium isopropoxide is mainly a monomer in nonpolar solvents [4]. It is prepared by treating titanium tetrachloride with isopropanol. Hydrogen chloride is formed as a coproduct [4].



Properties titanium isopropoxide reacts with water to deposit titanium dioxide: [5]



This reaction is employed in the sol-gel synthesis of TiO_2 -based materials in the form of powders or thin films. Typically water is added in excess to a solution of the alkoxide in an alcohol. The composition, crystallinity and morphology of the inorganic product are determined by the presence of additives (e.g. acetic acid), the amount of water (hydrolysis ratio), and reaction conditions [5]. The compound is also used as a catalyst in the preparation of certain cyclopropanes in the Kulinkovich reaction. Prochiral thioethers are oxidized enantioselectively using a catalyst derived from $\text{Ti} (\text{O-i-Pr})_4$ [6].

3.2.2 Acetic Acid

Acetic acid is the chemical compound responsible for the characteristic odor and sour taste of vinegar. Typically, vinegar is about 4 to 8% acetic acid. As the defining ingredient of vinegar, acetic acid has been produced and used by humans since before the dawn of recorded history. In fact, its name comes from the Latin for vinegar, acetum. Vinegar is formed from dilute solutions of alcohol, such as wine, by the action of certain bacteria in the presence of oxygen. These bacteria require oxygen, and the overall chemical change is the action of ethanol with oxygen to form acetic acid and water. $\text{CH}_3\text{CH}_2\text{OH} + \text{O}_2 \rightarrow \text{CH}_3\text{COOH} + \text{H}_2\text{O}$ The name, vinegar, comes from the French, VIN aigr, which means "sour wine." Nevertheless, vinegar may also be obtained from other fermented beverages such as malt or cider. Because vinegar is acidic, it has a variety of properties useful around the house. Mineral deposits left when hard water evaporates, such as those formed on plumbing fixtures and in tea kettles, dissolve in acids, so vinegar can be used to remove them. Because it is acidic, vinegar also inhibits the growth of bacteria, so vinegar is used as a preservative in foods, such as pickled vegetables, and as a mild disinfectant in cleaning. Of course, its sour taste, which is also a result of its acidity, makes it popular as a flavoring in cooking and in salad dressings. Pure acetic acid was first isolated about 1700 by the distillation of vinegar. When pure, acetic acid is a clear, colorless liquid with a sharp, irritating odor of vinegar. In poorly heated laboratories, the acid was often found frozen inside its container because its freezing point is only slightly below room temperature at 16.7°C . The term glacial (ice-like) came to be applied to the pure acid in either its solid or liquid state. Glacial acetic acid boils at 118°C , and has a density of 1.049 g/mL at 25°C . It is flammable with a flash point of 39°C . Through hydrogen-bonding interactions, acetic acid is miscible (mixable) in all proportions with water, ethyl alcohol, and diethyl ether. Pure or concentrated solutions of acetic acid are very corrosive and can cause painful burns. Aqueous solutions of acetic acid freeze at temperatures below the freezing point of water. For many years, the bulk of commercial acetic acid was produced by the oxidation of ethanol. Today, most industrial production of acetic acid is by the Monsanto process, in which carbon monoxide reacts with methanol under the influence of a rhodium complex catalyst at 180°C and pressures of 30–40 atm. $\text{CO} + \text{CH}_3\text{OH} \rightarrow \text{CH}_3\text{COOH}$ $[\text{Rh}(\text{CO})_2\text{I}_2]$

Acetic acid is classified as a weak acid, because it does not completely dissociate into its components when dissolved in aqueous solution. At a concentration of 0.1 M, only about 1% of the molecules are ionized. In solution, there is a dynamic equilibrium between the neutral molecules and the acetate and hydronium ions.

$\text{CH}_3\text{COH} + \text{H}_2\text{O} \rightleftharpoons \text{CH}_3\text{CO}^- + \text{H}_3\text{O}^+$. The acid dissociation constant (K_a value) for acetic acid is 1.8×10^{-5} at 25°C . Acetic acid is an important industrial chemical. About 3.2×10^9 kilograms of acetic acid were produced in the United States in 1999. The primary use of this chemical is in the manufacture of assorted acetate esters. These are substances formed by reacting acetic acid with a substance containing a hydroxyl ($-\text{OH}$) group.

3.2.3 Ethanol

The word alcohol denotes a fine powder of antimony produced by distilling antimony. Alcohol originally referred to any fine powder, but medieval alchemists later applied the term to the refined products of distillation, and this led to the current usage. Ethanol is a clear liquid alcohol that is made by the fermentation of different biological materials. This alcohol is known to have many uses, but one in particular is becoming more popular. Ethanol, the most widely used biofuel, is made in a process similar to brewing beer. The ethanol in the end is blended with gasoline to improve vehicle performance and reduce air pollution. Ethanol is a liquid alcohol that is manufactured by the fermentation of a wide variety of biological materials. Ethanol is best produced from lower value grains such as barley, corn and feed wheat. Higher value "bread" wheats would remain in ample supply for export sales, when Canada begins major ethanol manufacturing. Also, poor quality (weather damaged, immature) grains which are less suitable for either human or livestock use are excellent for ethanol production. Corn and starch based crops are the most common medium used in ethanol production. This indicates that once ethanol is in high demand, the prices of these crops will increase. For this reason other alternatives are being studied. Among these is the use of domestic cellulosic biomass feeds stocks such as herbaceous and woody plants, agricultural and forestry residues, and a large portion of municipal solid waste and industrial waste streams. Ethanol is miscible (mixable) in all proportions with water and with most organic solvents. It is useful as a solvent for many substances and in making perfumes, paints, lacquer, and explosives. Alcoholic solutions of nonvolatile substances are called

tinctures; if the solute is volatile, the solution is called a spirit. Commercial Alcohols have grown to be the largest manufacturer and supplier of industrial grade alcohol (ethyl alcohol or ethanol) in Canada. Its 1700 customers use the product in industrial applications (such as solvents, detergents, paints, printing inks, photo-chemical applications, latex processing, dyes, etc.), the beverage market, medicinal, pharmaceutical and food products and is the sole Canadian manufacturer and supplier to the fuel market in central and eastern Canada.

3.3 Methods

The three components were used in the preparation of the TiO_2 Sol-Gel sample are Titanium Isopropoxide (TIP) $\text{Ti}[\text{OCH}(\text{CH}_3)_2]_4$ purity 98%, Acetic acid CH_3COOH purity 99.5% and Ethanol $\text{CH}_3\text{CH}_2\text{OH}$ purity 99.7-100% all chemicals were as supplied local market. TIP is a metal alkoxide, where metal alkoxides have the general formula $\text{M}(\text{OR})_n$, where M=metal, R=alkyl group and n is the valence of the metal atom. TiO_2 sample is prepared by Sol-Gel method using 50 ml of Ethanol and allowed to mix for 50 min, measure 5 ml of acetic acid with a pipette into Ethanol and stir by using a magnetic stirrer it for 5 min or at least 3 min, and measure 6.3 ml of TIP was added by pipette to a beaker containing a mixture of glacial acetic acid and ethanol that had been mixed for five minutes. The mixture was continually stirred using a magnetic stirrer addition and for a further two minutes after addition of the precursor. These were thoroughly cleaned in Millipore water and neutral detergent for 10 min using an ultrasonic bath and then propanol was applied for further 10 min in the ultrasonic bath (type MXB14 sonic continuous of time from 0.1 to 99.9 min size 14 litter at temperature setting range 5-80 °C) (Grant). Put the solution in to a convenient glass beaker and seal it well. This sealing should keep the solution from contaminated air. Finally put the sample gel in the furnace at 600°C for 60 min, the sample be white powder (TiO_2).

3.4 Apparatus

3.4.1 X- Ray diffraction (XRD)

The X-ray powder diffractometer used in this work is a Bragg-Brentano type[65]. The essential features of such a diffractometer shown in Fig. (3.1).a powder sample C, placed on a flat plate, is supported on a table H, which can be rotated about an axis O which is perpendicular to the plane of drawing. The xray tube, S, emits a radiation, e.g, Cu K_{α} with $\lambda = 1.540598 \text{ \AA}$, with a line focal spot falling on the target T; S is also normal to the plane of drawing and therefore parallel to the diffractometer axis O. The special slit A is used to collimate the incident beam. The X- ray, which diverges from the source, is diffracted by the sample and afterwards forms a convergent diffracted beam which passes through the monochromator B and then is focused after the slit F and enters into the counter G. The receiving slits and detector are supported on the carriage E. The support E and H are mechanically coupled so that a rotation of the detector through 2θ degree is automatically accompanied by rotation of the sample through θ degrees. This coupling ensures that the angles of incidence on, and reflection from, the flat sample will always be equal to one another and equal to half the total angle of diffraction. The detector is connected to a computer-controlled pulse- processing electronic device. The whole computer-controlled set-up is driven by a program which enables one to initiate the data acquisition from a starting angle θ_i up to a final angle θ_f through a step of $\Delta\theta$ and with a dwell time of Δt . Then counting the intensity at each 2θ gives the sample diffractogram which, can be analyzed so as to obtain the structural properties of the sample under study.

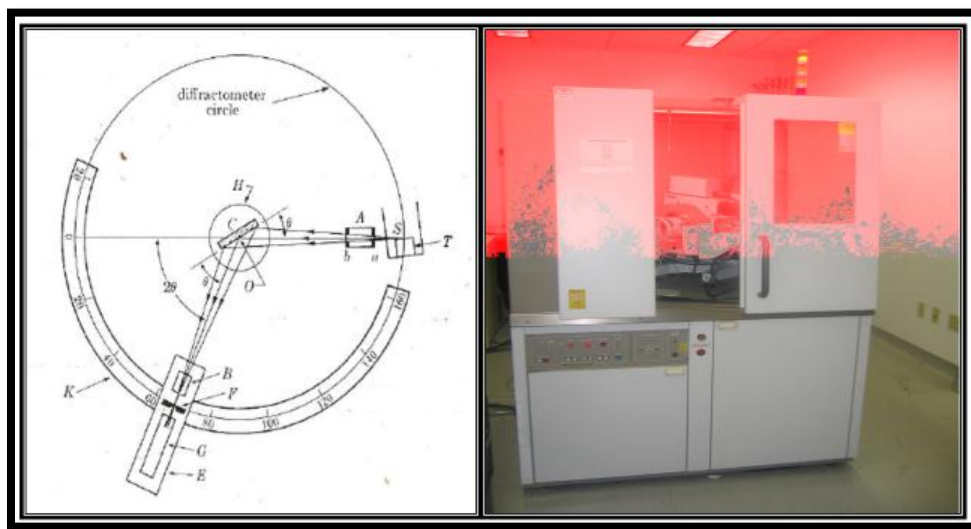


Fig (3.1): Schematic X-ray diffract meter of the Bragg-Brentano type.

The obtained mixed oxides for the samples were characterized by X-ray powder diffractometer using a continuous step scanning procedure (step size: 0.05° (in 2θ); time per step: 0.5 seconds), with a Bruker diffractometers and monochromatic $\text{Cu-K}\alpha$ radiation ($\lambda = 1.54064 \text{ \AA}$), using NaCl as an external calibration standard. The indexation of the powder diagrams and calculation of unit cell parameters were carried out using a locally modified version of the program Fullprof.

3.4.2 Infrared spectroscopy (FTIR)

Fourier transform infrared spectrometer (FTIR) is one of the important spectral techniques. An infrared spectrum represents a fingerprint of a sample with absorption peaks which correspond to the frequencies of vibrations between the bonds of the atoms making up the material, because each different material is a unique combination of atoms, no two compounds produce the exact same infrared spectrum. Therefore, infrared spectroscopy can be used for identification qualitative analysis of different materials [66]. The height of the peaks in the spectrum is a direct indication of the amount of material present. Infrared spectroscopy is an easy way to identify the presence of certain functional groups in a molecule. Also, one can use the unique collection of absorption bands to detect the presence of specific impurities.

Figure (3.2) is the schematic diagram and picture for FTIR

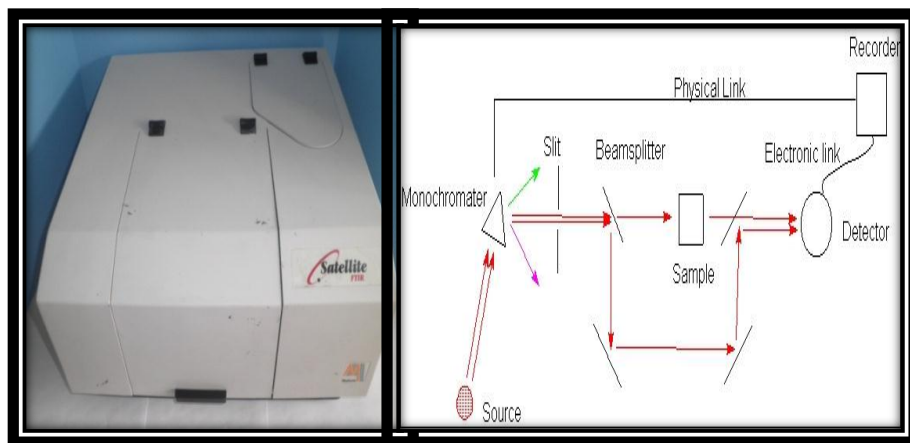


Fig (3.2): Continuous Wave spectrometers (FTIR).

A source of IR generates light across the spectrum of interest, A monochromatic (in IR this can be either a salt prism or a grating with finely spaced etched lines) separates the source radiation into its different wavelengths. A slit selects the collection of wavelengths that shine through the sample at any given time. In double beam operation, a beam splitter separates the incident beam in two; half goes to the sample, and half to a reference. The sample absorbs light according to its chemical properties. A detector collects the radiation that passes through the sample, and in double-beam operation, compares its energy to that going through the reference. The detector puts out an electrical signal, which is normally sent directly to an analog recorder. A link between the monochromatic and the recorder allows us to record energy as a function of frequency or wavelength, depending on how the recorder is calibrated. The infrared spectra were recorded with a FTIR instrument, using the KBr pellet technique [67].

3.5 Ultraviolet-visible spectrophotometer

The basic parts of a spectrophotometer are a light source, a holder for the sample, a diffraction grating in a monochromator or a prism to separate the different wavelengths of light, and a detector. The radiation source is often a Tungsten filament (300-2500 nm), a deuterium arc lamp, which is continuous over the ultraviolet region (190-400 nm), Xenon arc lamp, which is continuous from 160-2,000 nm; or more recently, light emitting diodes (LED) for the visible wavelengths. The detector is typically a photomultiplier tube, a photodiode, a photodiode array or a charge-coupled device (CCD). Single photodiode detectors and photomultiplier tubes are used with scanning monochromators, which filter the light so that only light of a single wavelength reaches the detector at one time. The scanning monochromator moves the diffraction grating to "step-through" each wavelength so that its intensity may be measured as a function of wavelength. Fixed monochromators are used with CCDs and photodiode arrays. As both of these devices consist of many detectors grouped into one or two dimensional arrays, they are able to collect light of different wavelengths on different pixels or groups of pixels simultaneously. A spectrophotometer can be either single beam or double beam. In a single beam instrument (such as the Spectronic 20), all of the light passes through the sample cell. I_0 must be measured by removing the sample. This was the earliest design and is still in common use in both teaching and industrial

labs. Samples for UV/Vis spectrophotometry are most often liquids, although the absorbance of gases and even of solids can also be measured. Samples are typically placed in a transparent cell, known as a cuvette. Cuvettes are typically rectangular in shape, commonly with an internal width of 1 cm. (This width becomes the path length, L , in the Beer-Lambert law.) Test tubes can also be used as cuvettes in some instruments. The type of sample container used must allow radiation to pass over the spectral region of interest. The most widely applicable cuvettes are made of high quality fused silica or quartz glass because these are transparent throughout the UV, visible and near infrared regions. Glass and plastic cuvettes are also common, although glass and most plastics absorb in the UV, which limits their usefulness to visible wavelengths[28]. Specialized instruments have also been made. These include attaching spectrophotometers to telescopes to measure the spectra of astronomical features. UV-visible micro spectrophotometers consist of a UV-visible microscope integrated with a UV-visible spectrophotometer. A complete spectrum of the absorption at all wavelengths of interest can often be produced directly by a more sophisticated spectrophotometer[29]. In simpler instruments the absorption is determined one wavelength at a time and then compiled into a spectrum by the operator. By removing the concentration dependence, the extinction coefficient (ϵ) can be determined as a function of wavelength. UV device that we used during our research is an automatic recording single beam spectrophotometer type UV Mini 1240 manufactured by Shimadzu company–Japan and coming with serial number A10934081718SM.



Fig (3.3): UV device that we used during our research.

3.6 Experiential One Synthesis and Cractrization TiO₂ Nanomaterial

Titanium Isopropoxide (TIP) $\text{Ti}[\text{OCH}(\text{CH}_3)_2]_4$ purity 98%, Acetic acid CH_3COOH purity 99.5% and Ethanol $\text{CH}_3\text{CH}_2\text{OH}$ purity 99.7-100% and all chemicals were supplied from local market. TIP is a metal alkoxide, where metal alkoxides have the general formula $\text{M}(\text{OR})_n$, where M=metal, R=alkyl group and n is the valence of the metal atom. TiO_2 sample are prepared by Sol-Gel method using 50 ml of Ethanol and allowed to mix for 50 min, then measure 5 ml of acetic acid with a pipette to be added into Ethanol and stir by using a magnetic stirrer it for 5 min or at least 3 min. Also measure 6.3 ml of TIP was added by pipette to a beaker containing a mixture of glacial acetic acid and ethanol that had been mixed for five minutes. The mixture was continually stirred using a magnetic for a further two minutes after addition of the precursor. These were thoroughly cleaned in Millipore water and neutral detergent for 10 min using an ultrasonic bath and then propanol was applied for further 10 min in the ultrasonic bath (type MXB14 sonic continuous of time from 0.1 to 99.9 min size 14 liter at temperature setting range 5-80 °C) (Grant). Put the solution in to a convenient glass beaker and seal it well. This sealing should keep the solution from contaminated air. Finally. Put the sample gel in the furnace at 600°C for 60 min, the sample will then be white powder (TiO_2). After preparation of TiO_2 one study the nano size material by X-ray diffractometer (XRD) and Scanning electronic microscopy (SEM). Then study the optical absorbance and determine some optical properties like (absorption coefficient, energy band gap, Refractive Index and Optical Conductivity). Moreover, the study was extended to characterize by UV-spectroscopy. Then use the infrared spectra for synthesizing TiO_2 nano powders by Mattson Fourier Transform Infrared Spectrophotometer (FTIR).

3.7 The effect of adding TiO₂ nanomaterial on the blood samples

Titanium dioxides (TiO_2) The (TiO_2) nano-particles dissolved in distilled water by ultrasonic for 5 min. Titanium dioxides (TiO_2) having concentrations (1, 2, 3, 4, 5, 6, 7 and 8) ppm were added to human blood to form 8 samples. These samples were kept concentration and examined for 4 weeks. Ultra violet spectro meter and the conventional medical tests were made weekly for 4 weeks.

3.8 The effect of adding TiO_2 to water on its physical properties

Titanium dioxides (TiO_2) having concentrations 0.1, 0.2, 0.3, 0.4, 0.5, 0.6, 0.7, and 0.8 ppm were added to water to form 8 samples. The PH of these samples were measured weekly for 4 weeks using PH meter. When TiO_2 was concentrations the number of living Escherihia E-coli cells in water for each concentration were determined weekly to up 4 weeks.

Chapter Four

Results and discussion

4.1 Introduction

After preparing TiO₂ sample optical, electrical and morphology properties were studied by using UV spectrometer beside, XRD technique, ESM and FTIR spectroscopy. The TiO₂ was added in different concentrations to the blood and water and their UV absorption and PH wear studied.

4.2 Results

4.2.1 Optical Results of TiO₂ sample

The following figures come from the absorption spectro UV.

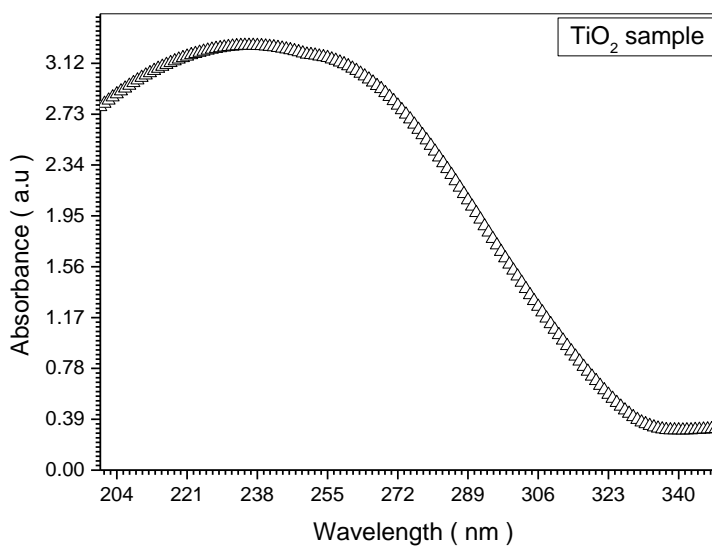
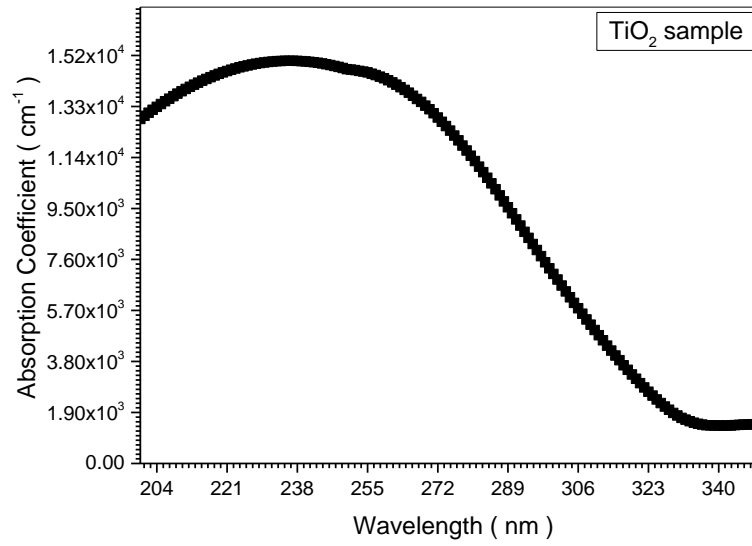
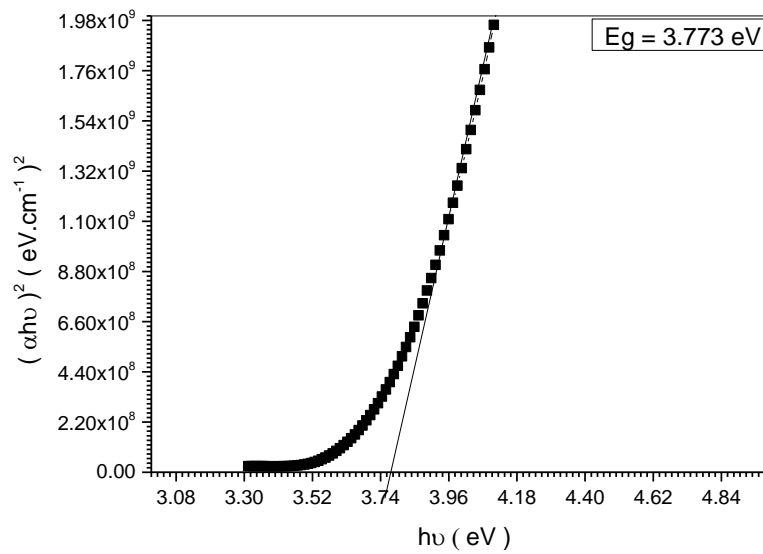


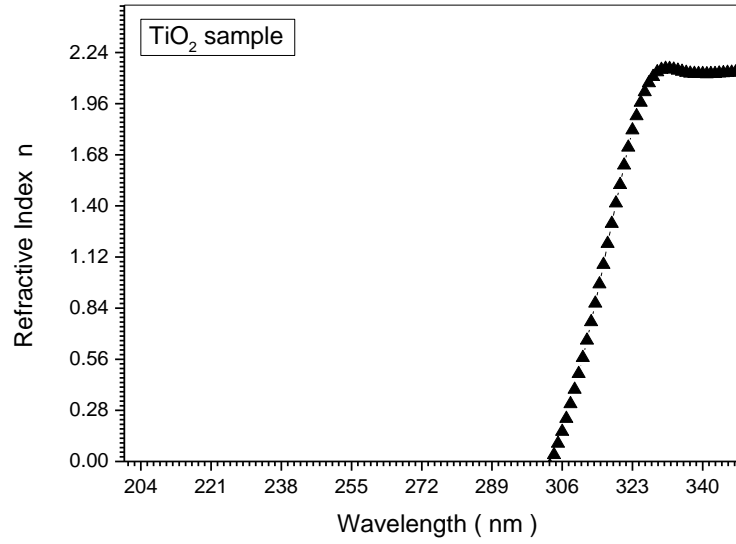
Fig (4.1) Relation between absorbance and wavelengths of TiO₂ sample.



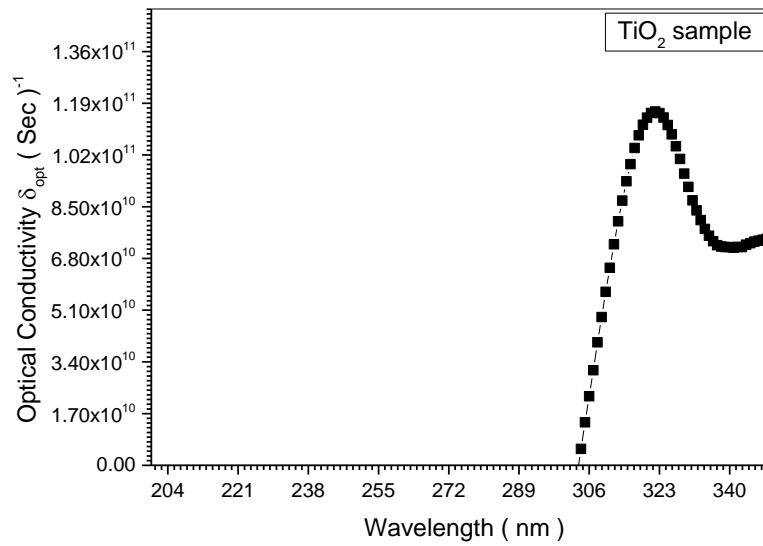
Fig(4.2) Relation between absorption coefficient α and wavelengths of TiO₂ sample.



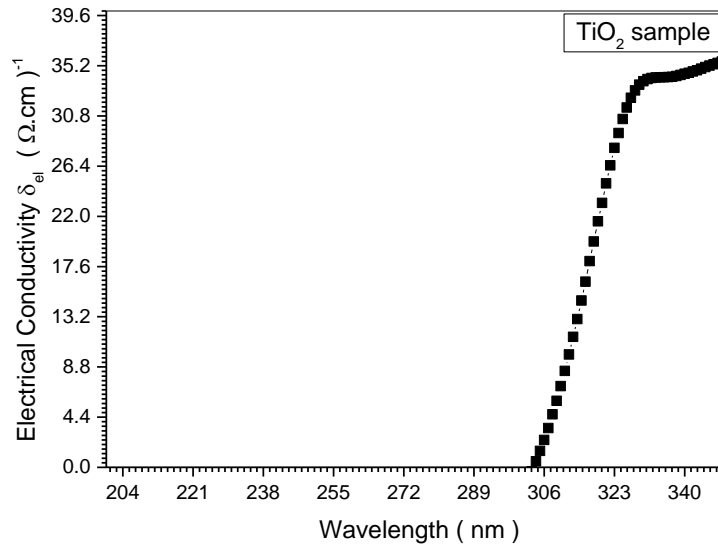
Fig(4.3) Optical energy band gap of TiO₂ sample.



Fig(4.4) Relation between refractive Index and wavelengths of TiO_2 sample.



Fig(4.5) Relation between optical conductivity and wavelengths of TiO_2 sample.



Fig(4.6) Relation between electrical conductivity and wavelengths of TiO_2 sample.

4.2.2 SEM Results of TiO_2 sample

The following figures results form SEM.

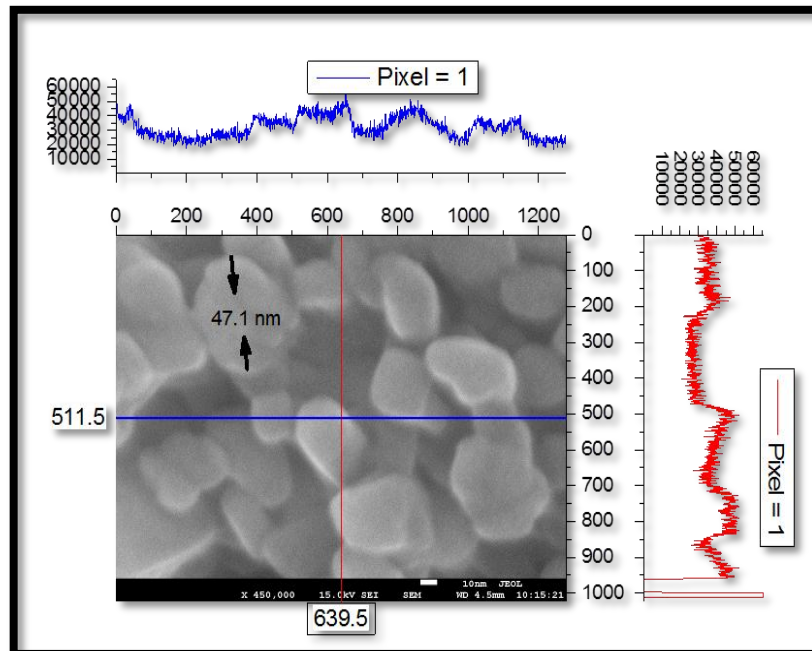


Fig (4.7) SEM image of TiO_2 .

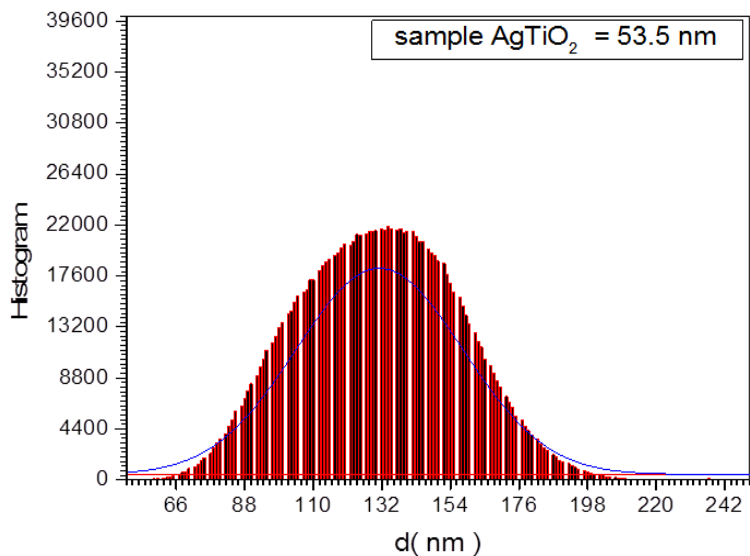


Fig (4.8) Histogram SEM image of TiO_2 .

4.2.3 XRD Results of TiO_2 sample

The following figures and tables result from XRD

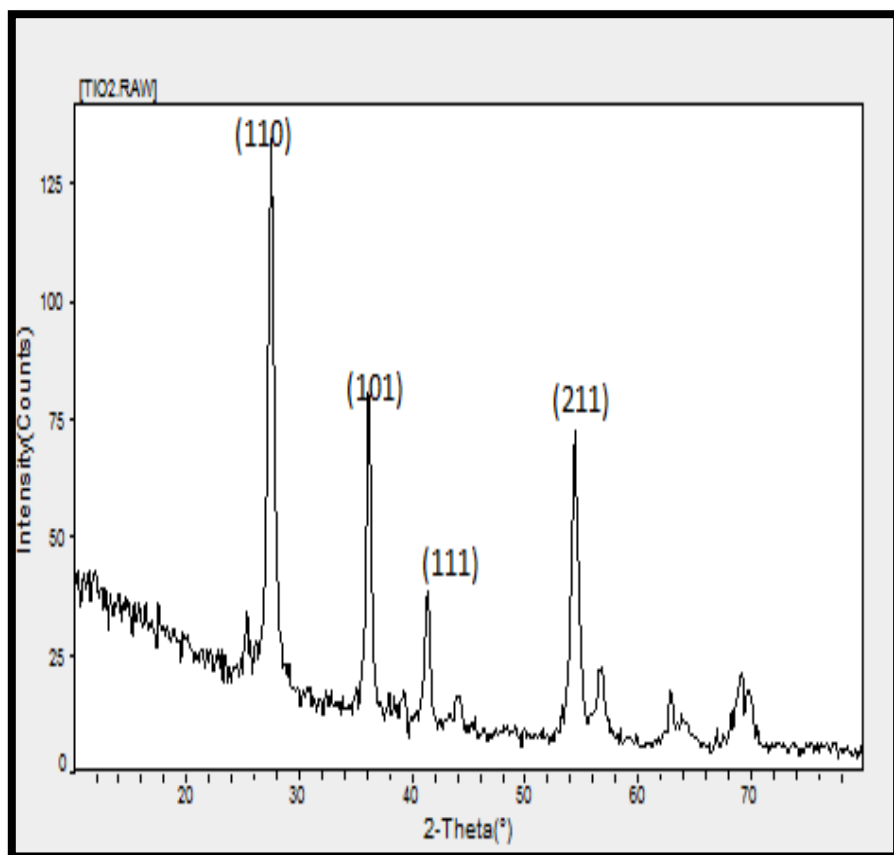


Fig (4.9) XRD spectrum of Nano TiO_2 sample.

Table (4.1) Lattice Constants from Peak Locations and Miller Indices [Tetragonal] of TiO₂ sample

2 θ	d (nm)	h k l	X _S (nm)
27.494	3.2458	1 1 0	45.3
36.125	2.4855	1 0 1	48.3
41.353	2.1839	1 1 1	53.6
54.393	1.6805	2 1 1	60.3

Average Lattice Constants = 4.8585

$$a = b = 4.585 \quad c = 2.964$$

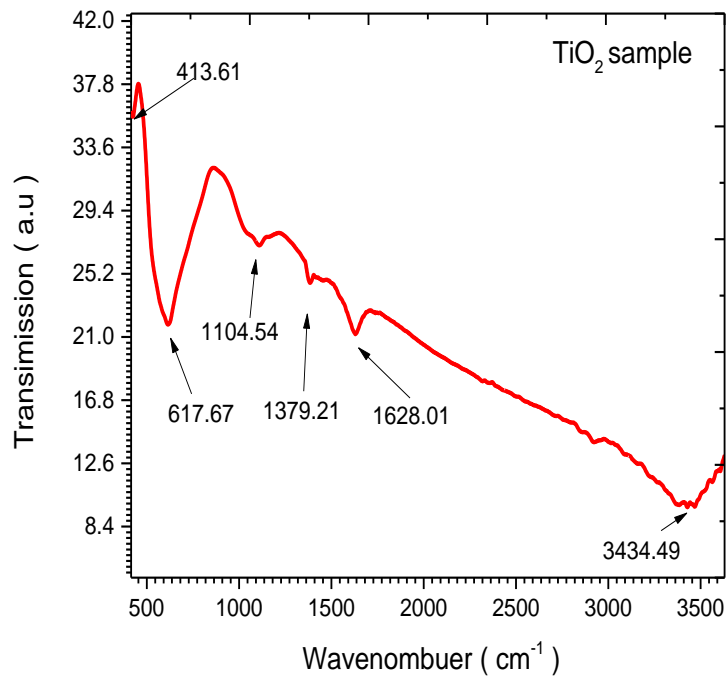
$$\alpha = \beta = \gamma = 90^\circ$$

$$\text{Density} = 4.2592 \text{ mg.cm}^{-3}$$

Crystal Form: Tetragonal – Primitive - Space Group: P42/mm (136)

4.2.4 FTIR Results of TiO₂ sample

The following figures and tables results from FTIR spectra



Fig(4.10) FTIR spectrum of TiO₂ sample.

Table (4.2) Parameters of T iO₂ sample

No	Wavenumber (cm ⁻¹)	Functional Group	Wavenumber (cm ⁻¹)	Functional Group
1	415	metal-oxygen	600–500	C-I stretch
2	620	metal-oxygen	700–600	C - Br stretch
3	1105	Methyl Formate	(1300-1000)	C-C stretch
4	1380	Methane	1400-1300	C =O Bond
5	1630	Methyl Formate	1755-1650	C=O Stretch
6	3440	Methanamide	3500-2400	Hydrogen- bonded O-H Stretch

4.2.5 Blood and TiO₂ Result

The following figures and tables results from UV spectra of blood samples weekly up to 4 weeks. Table (4.7) shows clinical examination of blood samples.

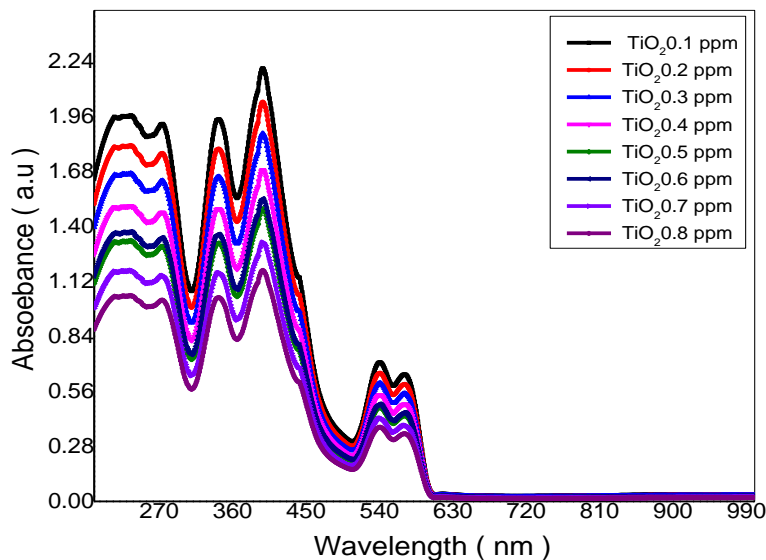
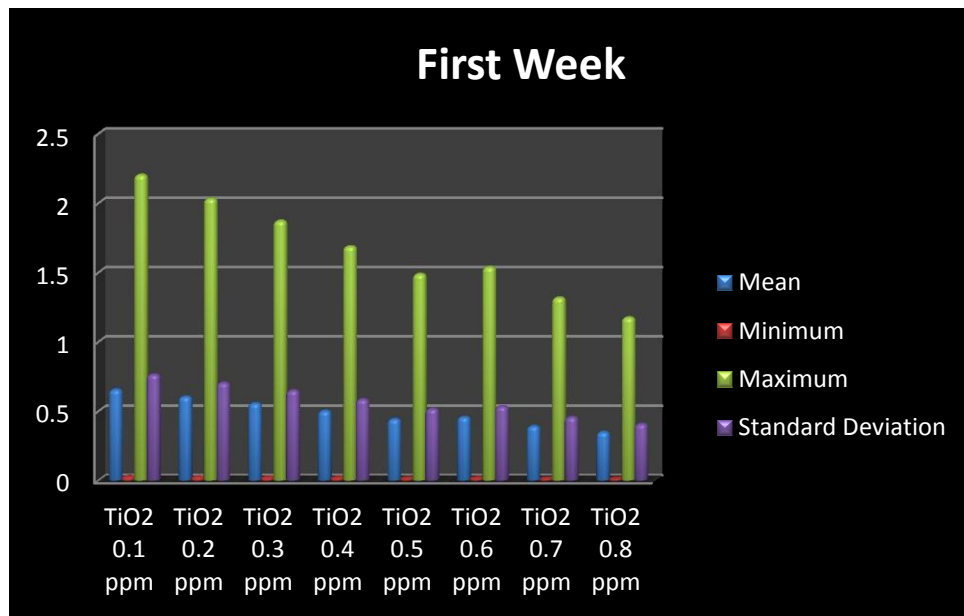


Fig (4.11) Absorption curves of blood samples that effects by TiO₂ with different concentration (0.1, 0.2, 0.3, 0.4, 0.5, 0.6, 0.7 and 0.8) ppm at First week.

Table (4.3) Absorption curves riding statically of blood sample by different concentration of TiO₂ at First week

Samples Absorbance	Mean	Minimum	Maximum	Standard Deviation
TiO ₂ – 0.1 ppm	0.65611	0.02706	2.20434	0.76488
TiO ₂ – 0.2 ppm	0.60504	0.02496	2.03277	0.70534
TiO ₂ – 0.3 ppm	0.55741	0.02299	1.87275	0.64982
TiO ₂ – 0.4 ppm	0.50251	0.02073	1.6883	0.58582
TiO ₂ – 0.5 ppm	0.4431	0.01828	1.4887	0.51656
TiO ₂ – 0.6 ppm	0.45824	0.0189	1.53956	0.53421
TiO ₂ – 0.7 ppm	0.3925	0.01619	1.31868	0.45756
TiO ₂ – 0.8 ppm	0.34999	0.01444	1.17587	0.40801

Fig



(4.12) Rated of statically absorption curves riding of blood sample by different concentration of TiO₂ at First week.

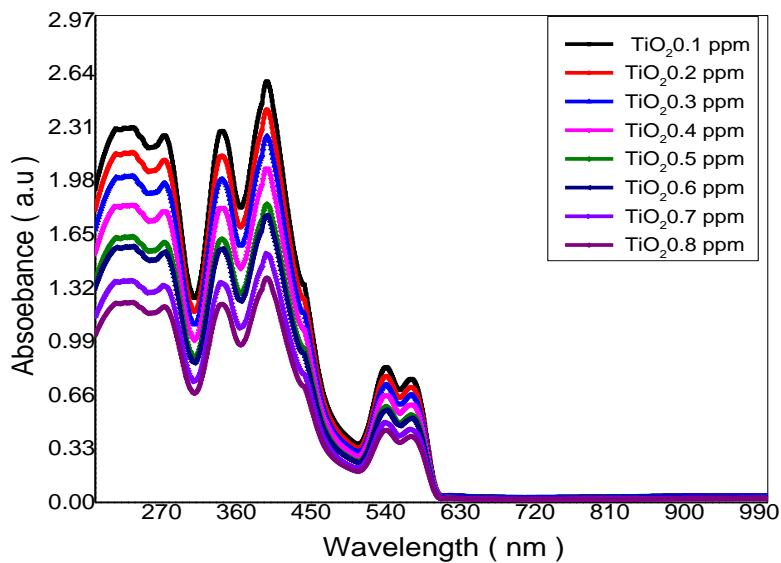


Fig (4.13) Absorption curves of blood samples that effects by TiO_2 with different concentration (0.1, 0.2, 0.3, 0.4, 0.5, 0.6, 0.7 and 0.8) ppm at Second week.

Table (4.4) Absorption curves riding statically of blood sample by different concentration of TiO_2 at Second week.

Samples Absorbance	Mean	Minimum	Maximum	Standard Deviation
$\text{TiO}_2 - 0.1$ ppm	0.7719	0.03184	2.59335	0.89986
$\text{TiO}_2 - 0.2$ ppm	0.72029	0.02971	2.41996	0.83969
$\text{TiO}_2 - 0.3$ ppm	0.67158	0.0277	2.25633	0.78291
$\text{TiO}_2 - 0.4$ ppm	0.61282	0.02528	2.0589	0.71441
$\text{TiO}_2 - 0.5$ ppm	0.54704	0.02257	1.8379	0.63773
$\text{TiO}_2 - 0.6$ ppm	0.52671	0.02173	1.76961	0.61403
$\text{TiO}_2 - 0.7$ ppm	0.45639	0.01883	1.53335	0.53205
$\text{TiO}_2 - 0.8$ ppm	0.41175	0.01699	1.38338	0.48001

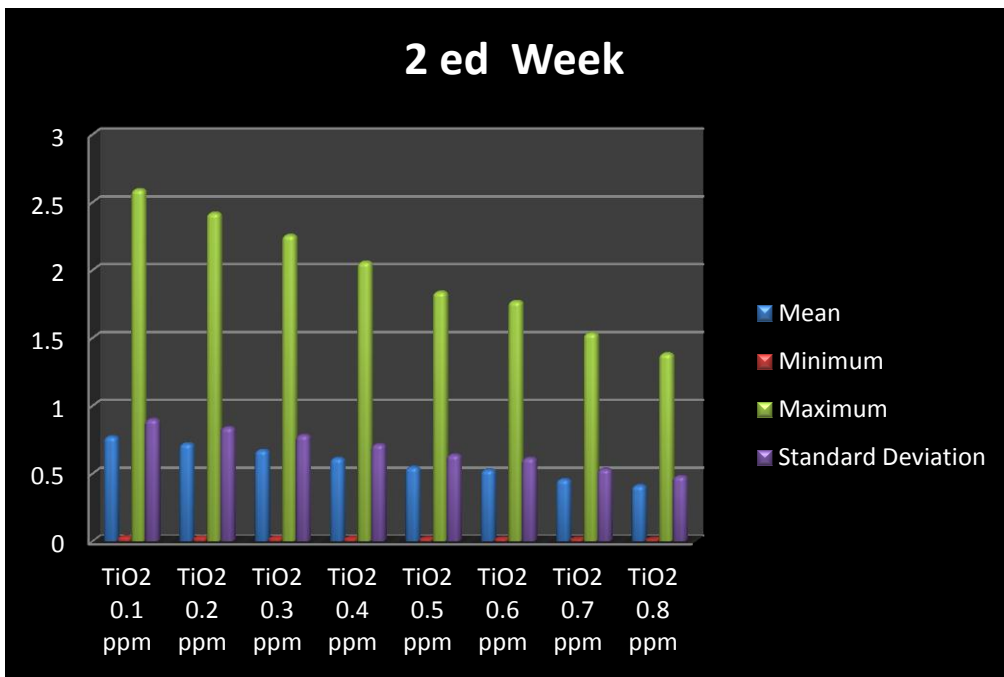


Fig (4.14) Absorption curves of blood samples that effects by TiO₂ with different concentration (0.1, 0.2, 0.3, 0.4, 0.5, 0.6, 0.7 and 0.8) ppm at Second week.

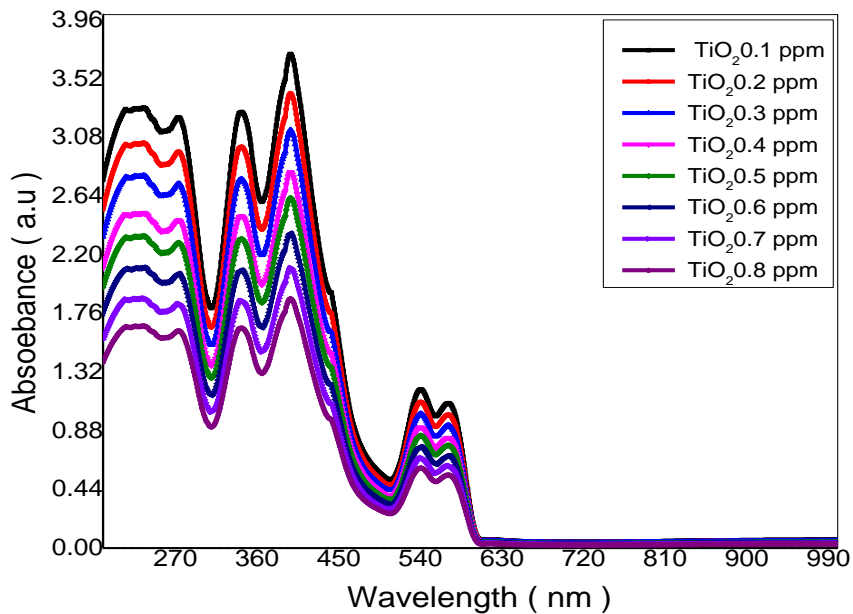


Fig (4.15) Absorption curves of blood samples that effects by TiO₂ with different concentration (0.1, 0.2, 0.3, 0.4, 0.5, 0.6, 0.7 and 0.8) at 3red week ppm.

Table (4.5) Absorption curves riding statically of blood sample by different concentration of TiO₂ at 3red week.

Samples Absorbance	Mean	Minimum	Maximum	Standard Deviation
TiO ₂ – 0.1 ppm	1.10271	0.04549	3.70478	1.28551
TiO ₂ – 0.2 ppm	1.01449	0.04185	3.4084	1.18267
TiO ₂ – 0.3 ppm	0.93276	0.03848	3.13379	1.08738
TiO ₂ – 0.4 ppm	0.83948	0.03463	2.82041	0.97864
TiO ₂ – 0.5 ppm	0.78149	0.03224	2.62557	0.91104
TiO ₂ – 0.6 ppm	0.70229	0.02897	2.35948	0.81871
TiO ₂ – 0.7 ppm	0.6252	0.02579	2.10048	0.72884
TiO ₂ – 0.8 ppm	0.55643	0.02295	1.86943	0.64867

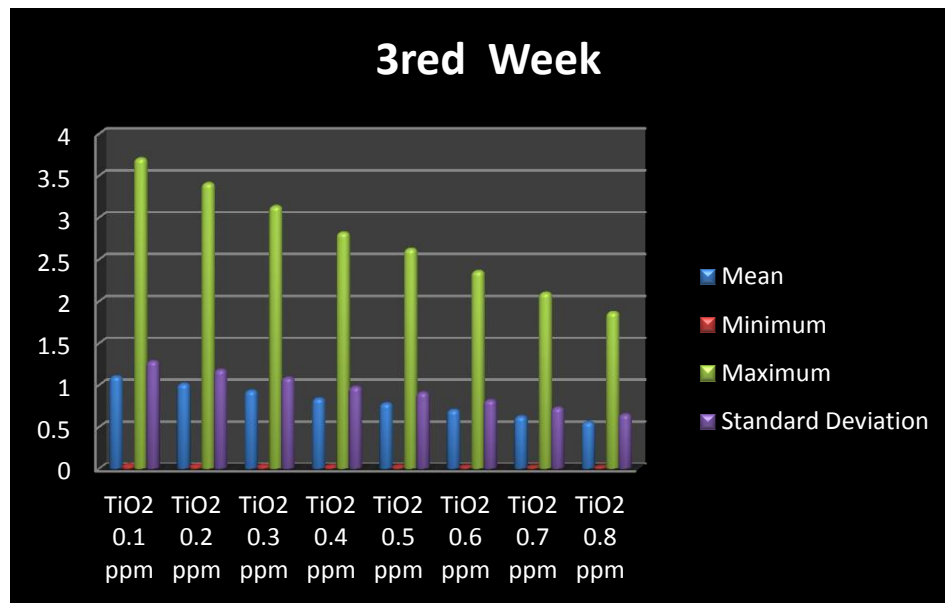


Fig (4.16) Rated of statically absorption curves riding of blood sample by different concentration of TiO₂ at 3red week.

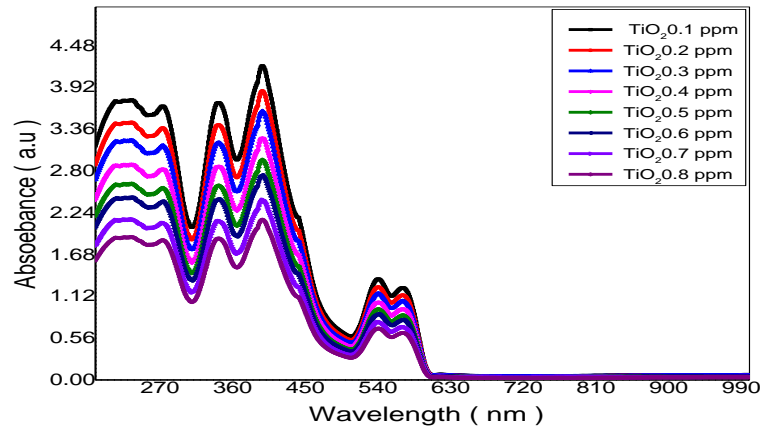


Fig (4.17) Absorption curves of blood samples that effects by TiO_2 with different concentration (0.1, 0.2, 0.3, 0.4, 0.5, 0.6, 0.7 and 0.8) ppm at Last week.

Table (4.6) absorption crves riding statically of blood sample by different concentration of TiO_2 at Last week

Samples Absorbance	Mean	Minimum	Maximum	Standard Deviation
$\text{TiO}_2 - 0.1$ ppm	1.25308	0.05169	4.20998	1.4608
$\text{TiO}_2 - 0.2$ ppm	1.15283	0.04755	3.87318	1.34394
$\text{TiO}_2 - 0.3$ ppm	1.07213	0.04423	3.60206	1.24986
$\text{TiO}_2 - 0.4$ ppm	0.96492	0.0398	3.24185	1.12488
$\text{TiO}_2 - 0.5$ ppm	0.87808	0.03622	2.95008	1.02364
$\text{TiO}_2 - 0.6$ ppm	0.81661	0.03369	2.74358	0.95198
$\text{TiO}_2 - 0.7$ ppm	0.71862	0.02964	2.41435	0.83775
$\text{TiO}_2 - 0.8$ ppm	0.63957	0.02638	2.14877	0.74559

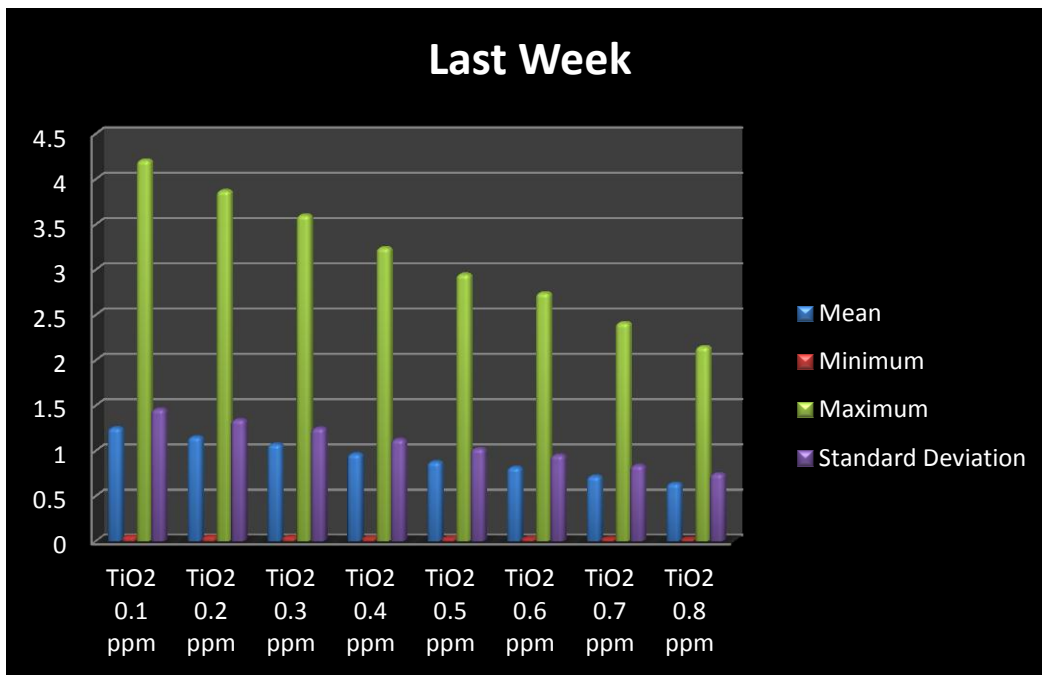


Fig (4.18) Rated of statically absorption curves riding of blood sample by different concentration of TiO_2 at Last week.

Table (4.7) Clinical examination of blood sample by different concentration of TiO₂

	Concentration of TiO ₂ for							
Sample	1 0.1	2 0.2	3 0.3	4 0.4	5 0.5	6 0.6	7 0.7	8 0.8
CBC test								
First Week								
RBC 10 ⁶ / μL	7.13	5.18	5.2	5.02	4.86	4.96	4.86	4.7
WBC10 ³ / μL	2.80	2.48	2.55	2.72	2.71	2.70	5.07	5.21
HGB g/dL	21.6	15.3	15.6	14.9	14.1	14.2	14.0	13.9
PLT10 ³ / μL	153	148	150	149	167	160	183	215
HCT %	60.6	43.2	43.8	42.9	41.1	42.2	42.4	39.5
MCV fL	85.0	83.5	83.2	85.6	84.7	85.1	83.7	84.0
MCH pg	30.2	29.5	29.6	29.6	29.0	28.6	27.6	29.5
MCHC g / μL	35.6	35.4	35.6	34.7	34.3	33.0	33.0	35.0
RDW	9.6	9.4	9.4	9.9	9.0	9.5	8.5	10.3
Second Week								
RBC 10 ⁶ / μL	5.56	5.43	5.52	5.37	5.10	5.1	5.2	4.95
WBC10 ³ / μL	2.29	2.24	2.50	2.5	1.62	1.4	1.88	4.31
HGB g/dL	16.3	15.5	15.4	15.0	14.5	14.4	14.4	14.0
PLT10 ³ / μL	360	145	280	128	191	167	175	183
HCT %	47.6	46.4	47.3	46.9	42.8	42.8	44.2	42.0
MCV fL	85.7	85.5	85.7	87.5	84.0	84.0	84.1	84.9
MCH	29.3	28.5	27.8	28.8	28.4	27.6	27.3	28.2
MCHC g / μL	34.2	33.4	32.5	33.0	33.0	32.9	32.5	33.0
RDW	11.2	11.2	10.9	11.0	10.0	10.8	10.6	10.7
Third Week								
RBC 10 ⁶ / μL	5.21	5.25	5.3	5.18	5.06	5.03	5.29	4.65
WBC10 ³ / μL	1.93 L	2.03	2.30	1.90	1.16	1.03	1.21	2.83
HGB g/dL	15.8	15.2	15.2	15.3	14.1	14.0	14.0	13.8
PLT10 ³ / μL	211	152	121	126	170	160	164	160
HCT %	44.9	45.4	46.7	45.3	43.6	42.4	45.5	40.0
MCV fL	86.3	86.6	86.7	87.5	86.2	84.3	86.1	86.2
MCH	30.3	28.9	28.2	29.5 p	27.8	27.8	26.4	29.6
MCHC g / μL	35.1	33.4	32.5	33.7	32.3	33.0	30.7	34.5
RDW	10.7	11.0	11.7	11.2	10.0	10.1	10.7	11.3
Forth Week								
RBC 10 ⁶ / μL	5.30	5.57	5.32	5.36	5.11	4.82	4.90	4.76
WBC10 ³ / μL	1.31	1.54	1.61	1.77	0.91	0.98	1.05	2.37
HGB g/dL	16.3	15.3	15.5	15.6	14.4	14.2	14.4	13.8
PLT10 ³ / μL	287	156	151	139	138	130	124	97
HCT %	45.5	47.8	45.4	46.8	43.6	39.9	41.6	40.0
MCV fL	86.0	85.9	85.5	87.4	85.4	82.9	84.9	84.2
MCH	30.7	27.4	29.1	29.1	28.1	29.6	29.3	28.9
MCHC g / μL	35.8	32.0	34.1	33.3	33.0	35.8	34.6	34.5
RDW	11.6	11.2	12.1	10.1	10.7	11.0	10.6	10.4

4.2.6 Escherichia coli water and TiO₂ results

The number of living Escherichia E-coli inside water samples having TiO₂ concentrations 0.1, 0.2 ... and 0.8ppm weekly for 4 weeks were determined.

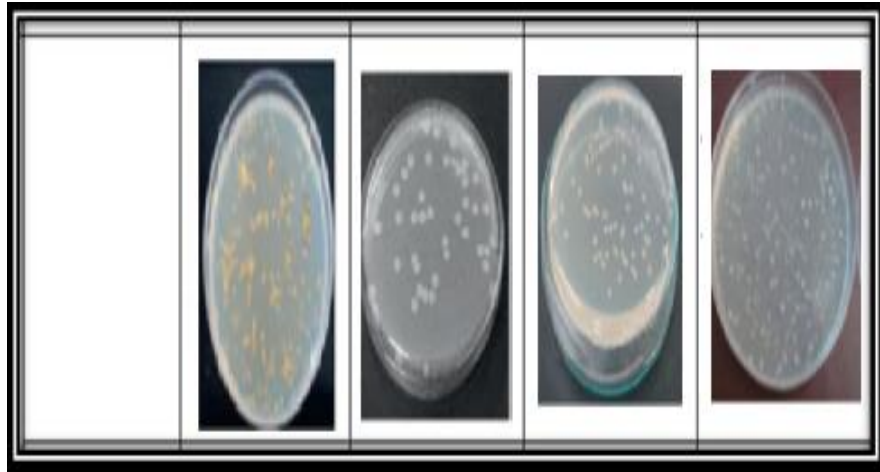


Fig (4.19) Effect of 0.1 ppm TiO₂ on the survival of number of viable cells Escherichia coli (CFU/ml) after 4 weeks on the water.

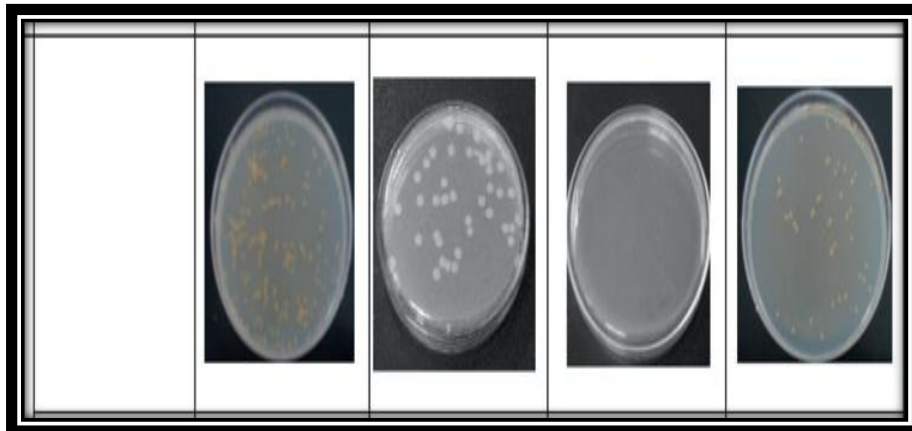


Fig (4.20) Effect of 0.2 ppm TiO₂ on the survival of number of viable cells Escherichia coli (CFU/ml) after 4 weeks on the water.

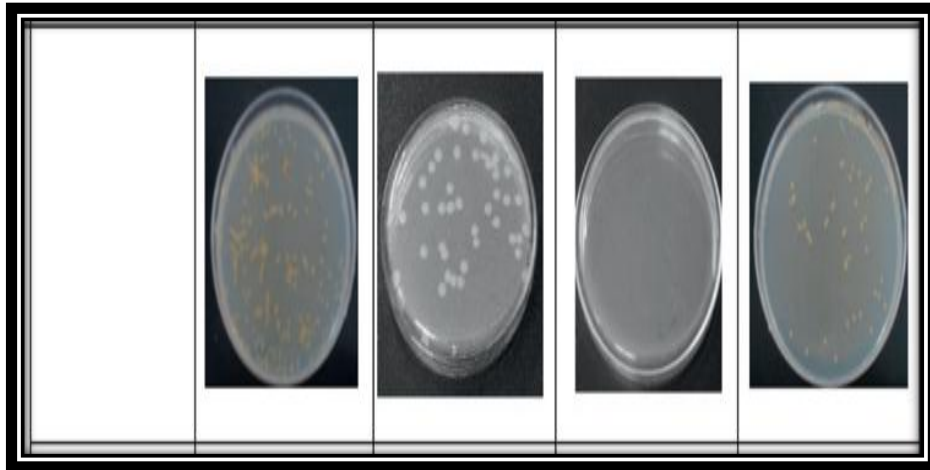


Fig (4.21) Effect of 0.3 ppm TiO₂ on the survival of number of viable cells *Escherichia coli* (CFU/ml) after 4 weeks on the water.

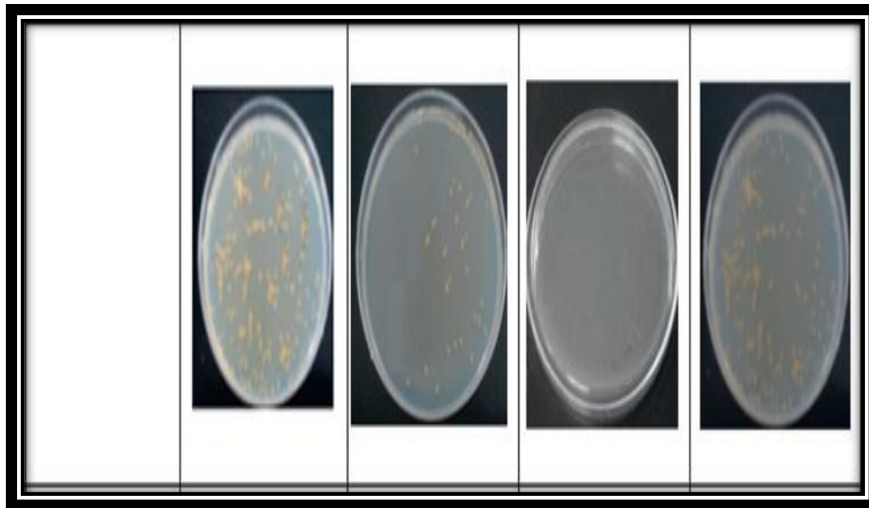


Fig (4.22) Effect of 0.4 ppm TiO₂ on the survival of number of viable cells *Escherichia coli* (CFU/ml) after 4 weeks on the water.

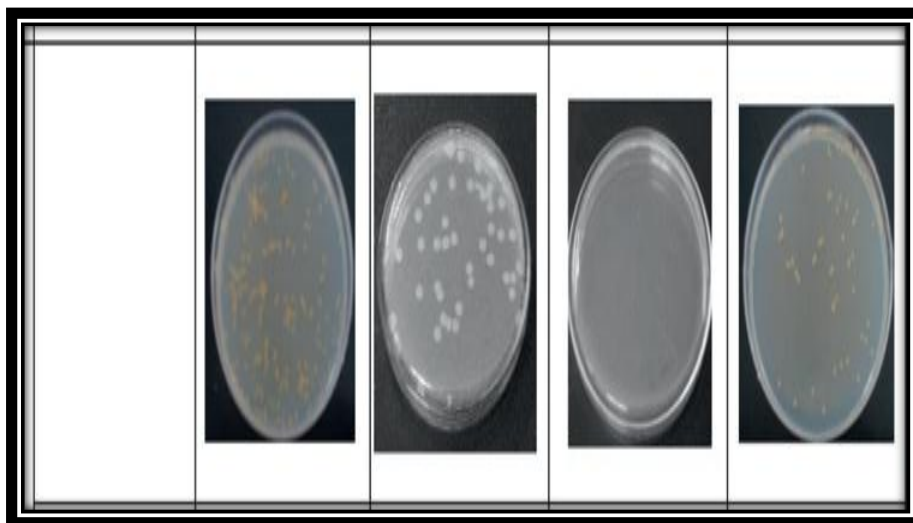


Fig (4.23) Effect of 0.5 ppm TiO₂ on the survival of number of viable cells *Escherichia coli* (CFU/ml) after 4 weeks on the water.

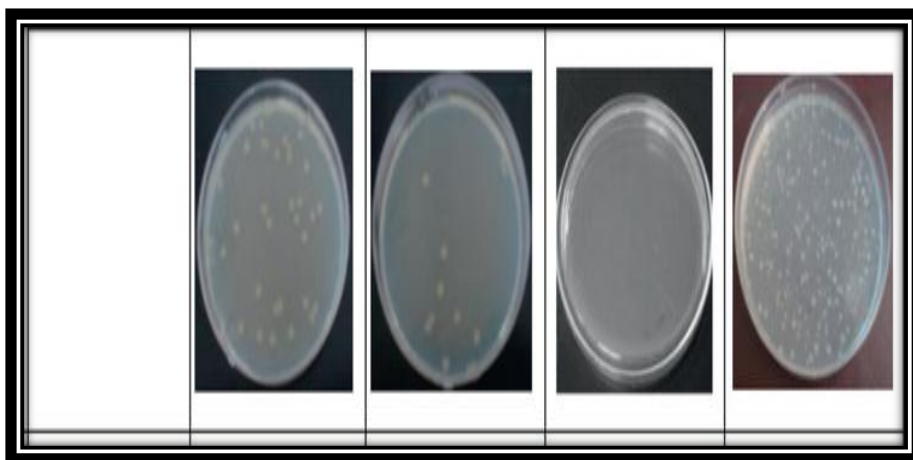


Fig (4.24) Effect of 0.6 ppm TiO₂ on the survival of number of viable cells *Escherichia coli* (CFU/ml) after 4 weeks on the water.

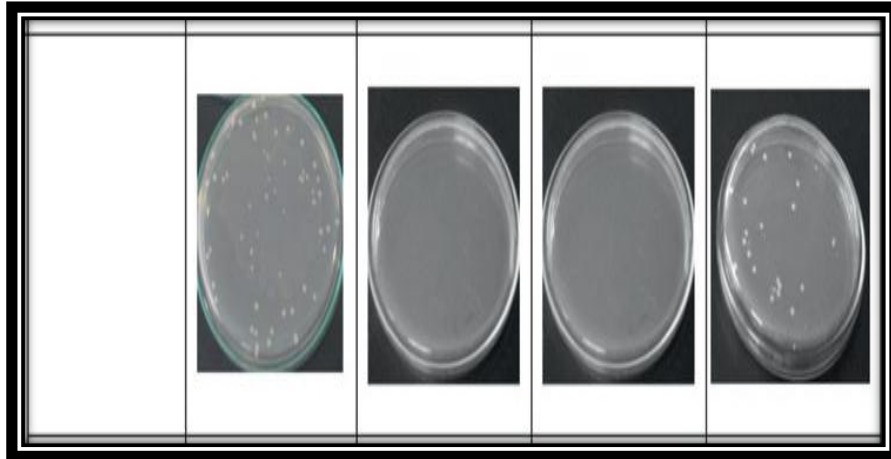


Fig (4.25) Effect of 0.7 ppm TiO₂ on the survival of number of viable cells *Escherichia coli* (CFU/ml) after 4 weeks on the water.

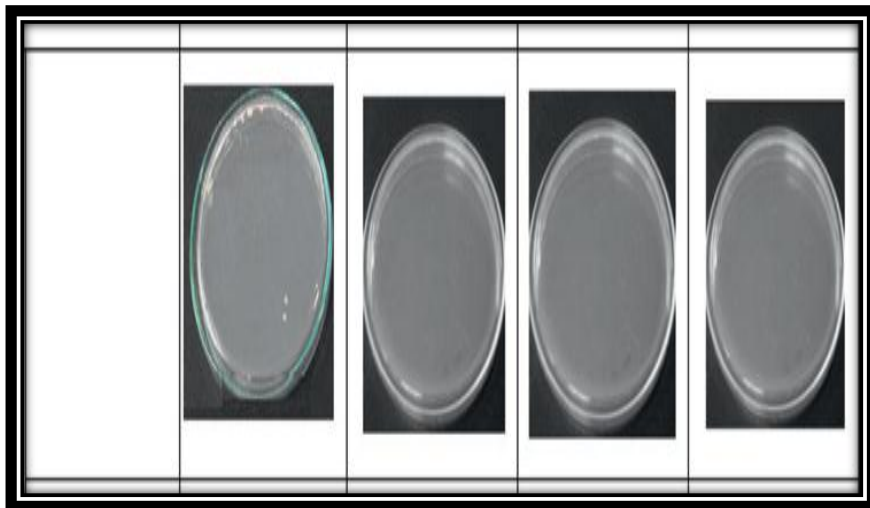


Fig (4.26) Effect of 0.8 ppm TiO₂ on the survival of number of viable cells *Escherichia coli* (CFU/ml) after 4 weeks on the water.

Table (4.8) the effect of TiO₂ on the survival of number of viable cells Escherichia coli (CFU/ml) after 4 weeks on the water.

Samples of water	C	First Week	Second Week	Thread Week	Fourths Week
Sample 1	0.1	4.75x10 ²	4.21x10 ²	3.83x10 ²	2.95x10 ²
Sample 2	0.2	4.64x10 ²	2.63x10 ²	2.24x10 ²	1.95x10 ²
Sample 3	0.3	4.52x10 ²	2.41x10 ²	2.12x10 ²	1.83x10 ²
Sample 4	0.4	4.48x10 ²	2.21x10 ²	2.05x10 ²	1.73x10 ²
Sample 5	0.5	4.29x10 ²	1.93x10 ²	1.81x10 ²	1.52x10 ²
Sample 6	0.6	4.13x10 ²	1.72x10 ²	1.69x10 ²	1.46x10 ²
Sample 7	0.7	4.05x10 ²	1.54x10 ²	1.34x10 ²	1.23x10 ²
Sample 8	0.8	4.02x10 ²	1.36x10 ²	1.24x10 ²	0.95x10 ²

C=Con centration of TiO₂

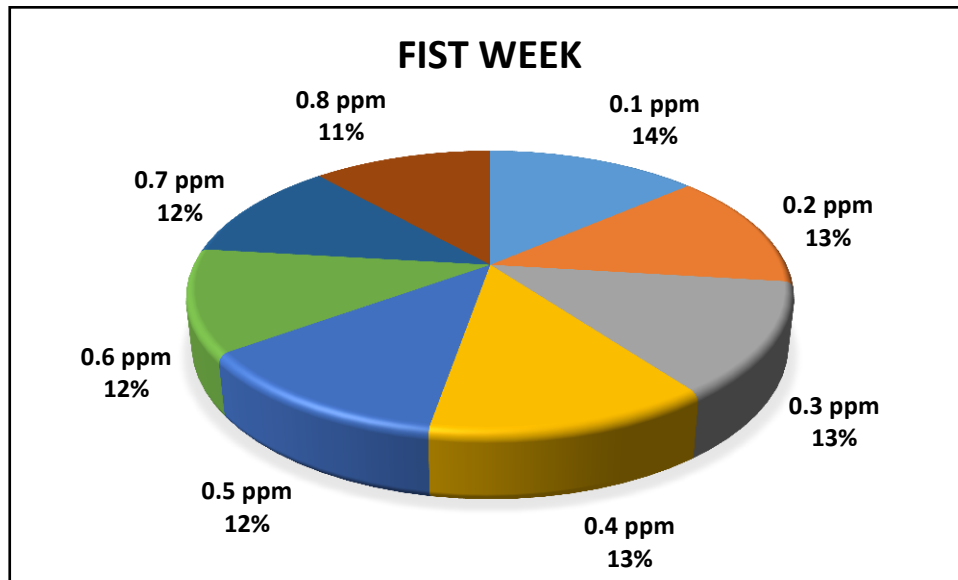


Fig (4.27) Effect of TiO₂ on the survival of number of viable cells Escherichia coli (CFU/ml) at first week.

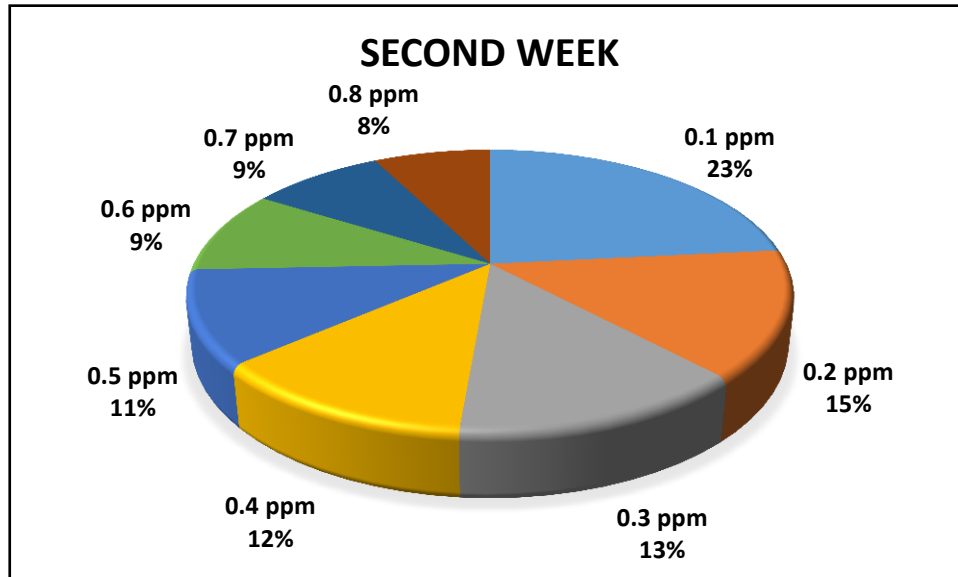


Fig (4.28) Effect of TiO₂ on the survival of number of viable cells Escherichia coli (CFU/ml) at second week.

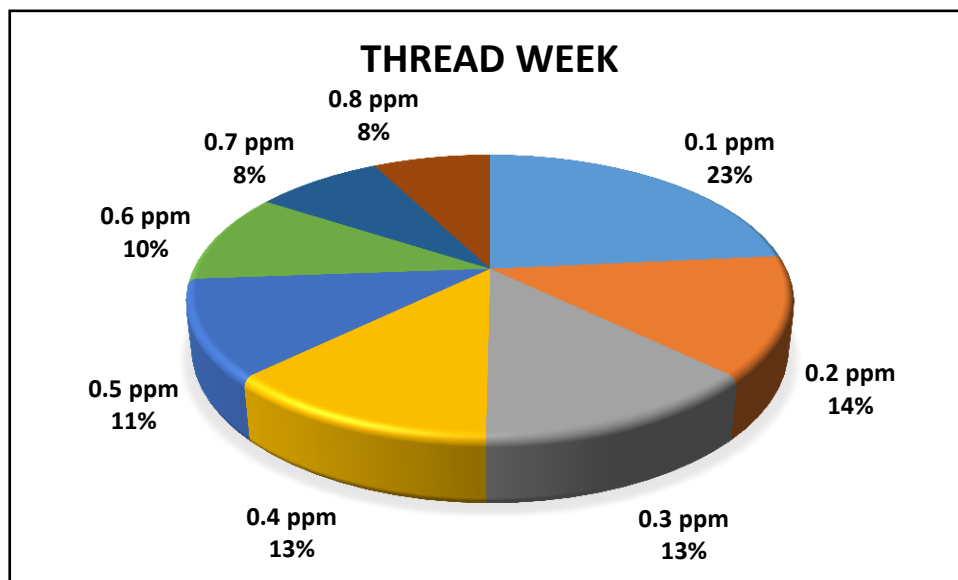


Fig (4.29) Effect of TiO₂ on the survival of number of viable cells Escherichia coli (CFU/ml) at thread week.

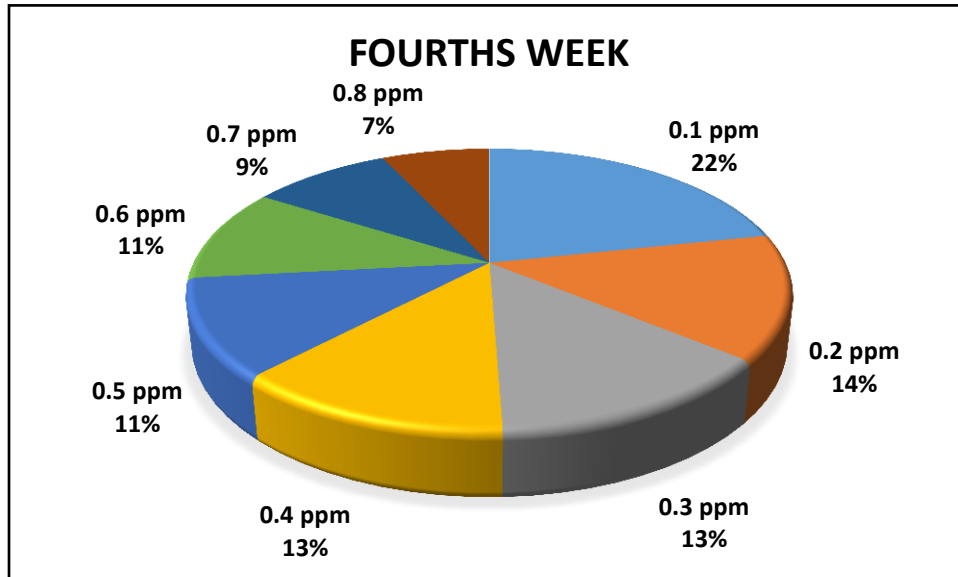


Fig (4.30) Effect of TiO₂ on the survival of number of viable cells Escherichia coli (CFU/ml) at last week.

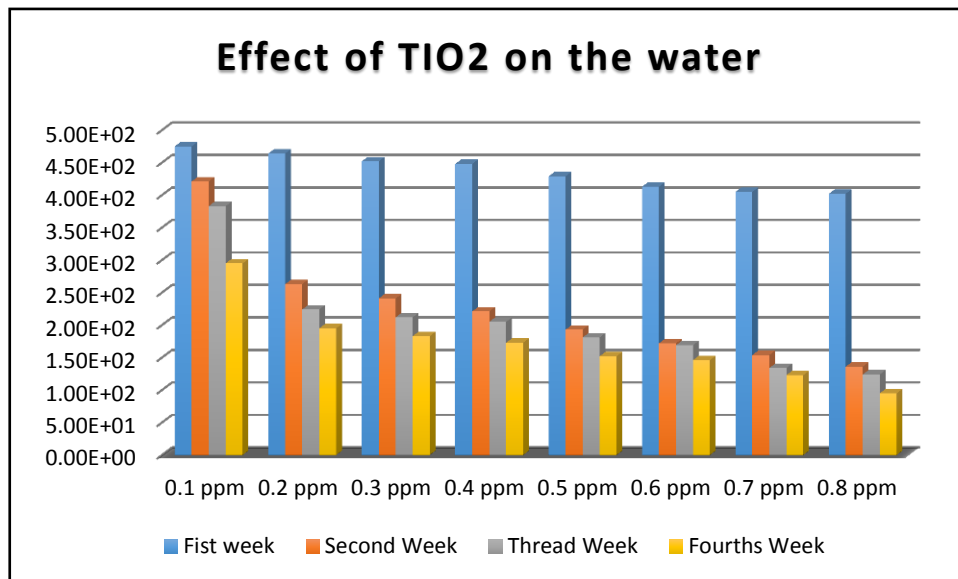


Fig (4.31) Effect of TiO₂ on the survival of number of viable cells Escherichia coli (CFU/ml) after 4 weeks.

Table (4.9) change of water PH with TiO_2 concentration and time.

	First Week pH	Second Week pH	Third Week pH	Fourth Week pH
Sample 0	14.75	12.21	11.83	9.95
Sample 1	14.64	11.63	10.24	8.95
Sample 2	14.52	10.41	9.12	8.83
Sample 3	14.48	10.21	8.05	7.73
Sample 4	14.29	9.93	7.81	7.52
Sample 5	14.13	8.72	7.69	6.46
Sample 6	14.05	8.54	7.34	6.23
Sample 7	14.02	7.36 ²	6.24	5.95

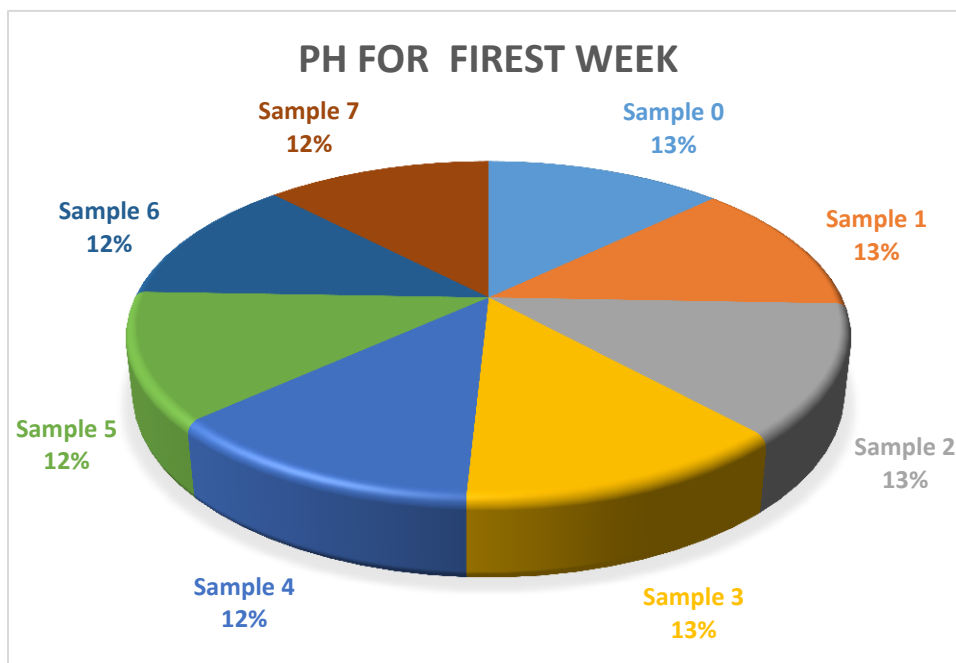


Fig (4.32) Effect of TiO_2 on the survival pH meter of viable cells Escherichia coli (CFU/ml) at first week.

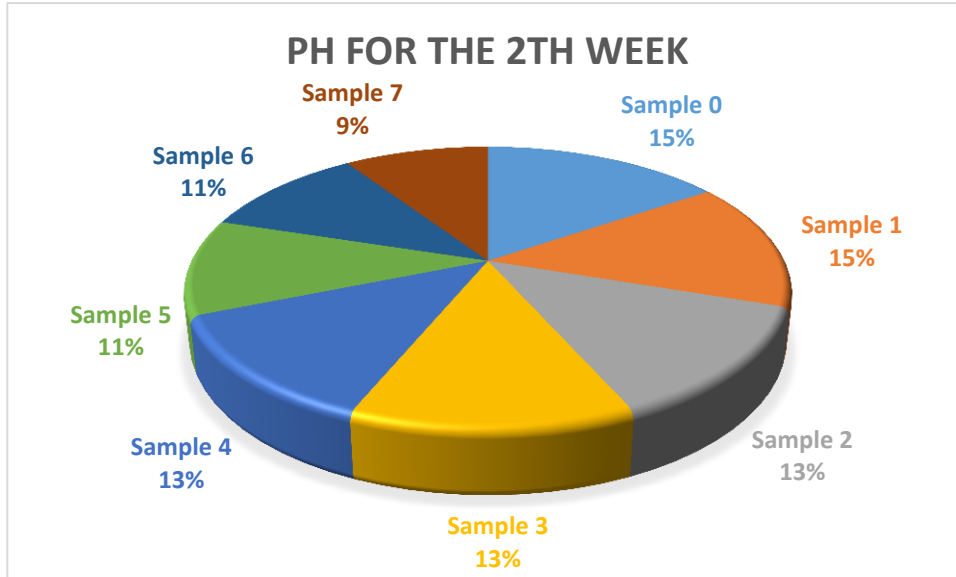


Fig (4.33) Effect of TiO₂ on the survival pH meter of viable cells Escherichia coli (CFU/ml) at second week.

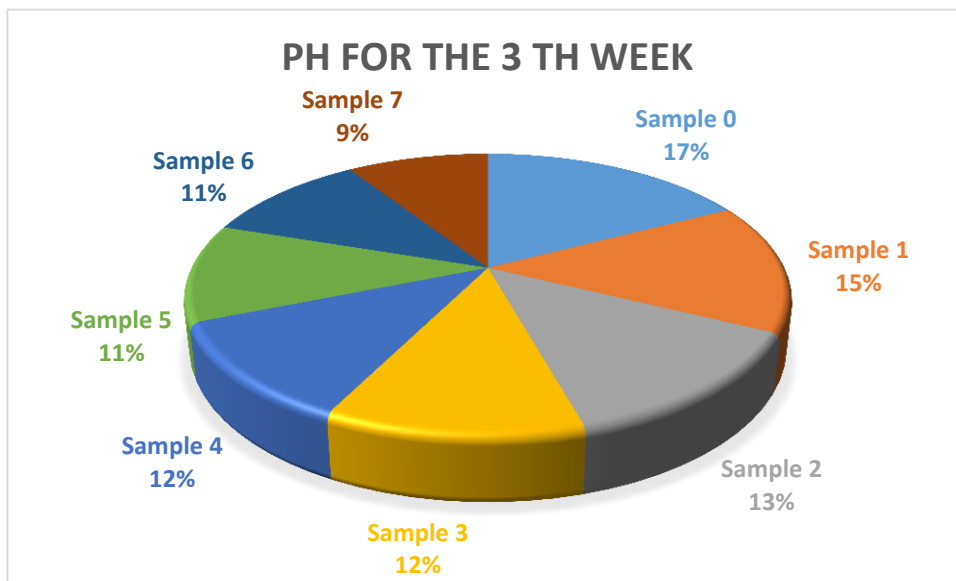


Fig (4.34) Effect of TiO₂ on the survival pH meter of viable cells Escherichia coli (CFU/ml) at therade week.

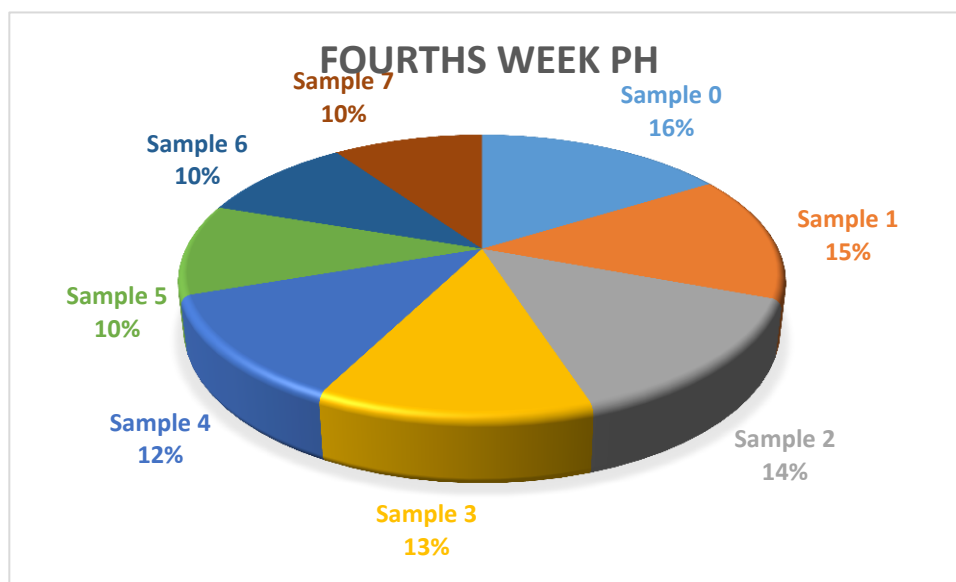


Fig (4.35) Effect of TiO₂ on the survival pH meter of viable cells Escherichia coli (CFU/ml) at first week.

4.3 Discussion

The optical properties of TiO₂ shown in figures (4.1, 2, 3, 4, 5 and 6) shows maximum absorption peak at about 238nm wave length with energy gap about 3.75eV. Sudden increase at wave length about 306nm. The SEM result shown in figure (4.8) indicates a wide variety of nano size of TiO₂ nano particles ranging from about 60 nm up to about 200 nm. However the XRF table (5.1) results show the particle sizes ranging from 45.3 nm up to about 60.3 nm. The smallness of XRF results may be related to the fact that XRF is more sensitive than SEM covers the whole surface thus scan very large number of nano particles, while XRF gives the crystal size of the particles that reflect the very narrow incident X-Ray. The FTIR result for TiO₂ figure (4.10) and table (4.2) shows existence of C-I, C-Br, C-C, C=O and O-H stretchings. The blood results in figures (4.11, 12, 13, 14, 15, 16, 17 and 18) indicates that increasing TiO₂ concentration decreases absorbance. For a certain concentration the absorbance increases with time. The decrease of absorbance accompanied with the increase of TiO₂ concentration may be related to the action of TiO₂ of decomposing blood compounds having high absorbance while the increase of absorbance with time may be attributed to the evaporation of compounds having high

absorbance with time. Table (4.7) shows also some interesting results. In general RBC and HCT counts or concentrations decrease in general up on increasing TiO_2 concentration. As far as the HCT is directly proportional to the viscosity too decrease. In general RBC and HCT counts or concentrations decrease with time up to the third week. Table (4.8) indicates that the number of viable living cells of E-coli decreases.

Up on increasing TiO_2 concentration and time. Thus decreasing water PH decreases the number of living cells. In other words increasing water PH increases the number of living cells. In other words increasing the number of living cells.

4.4 Conclusion

The TiO_2 tests show that it is in the form of nano powder having nano sizes ranging from about 45nm up to 200nm. The nano concentration of TiO_2 affects the blood and water properties. The blood absorbance decreases when TiO_2 concentration increases. The same holds for RBCs, HCT and blood viscosity where PH and the number of living E-coli cells increase up on decreasing TiO_2 nano concentration.

4.5 Future work

- 1- The blood and water physical properties can be studied in ranges below or above the range (0.1-0.8ppm).
- 2- Other physical properties of blood and water like magnetic and electric permittivity beside heat transfer coefficient can be also studied.
- 3- The properties of other photo nano catalysts need to be also studied.

References

- [1] Andrew M, Childs and win Vas dam, Quantum algorithms for. Rev. Mod. Physics, V. 82, 155.1.15 algebraic problems jjan. (2010)
- [2] Development of concepts in the history of quantum theory, 43 (5): A389-394 American journal of physics. (2010)
- [3] R Feynman, R.B Leighton, M. Sandi, ISBN0-201-02118-8 Feynman lectures on physics (Vol. 3), Addison Wesley. (2000)
- [4] Journals- Phys. RevB, Volume 38, Issue I- Functional integral theories of low dimensional quantum hesenber. (1999)
- [5] Iudovico, Anna. Effector Heisenberg. La rivoluzione scientific la storia. P. 224. ISBN 88- 8358-182-2 Roma. Armando. (2001)
- [6] P Chandra, P Coleman and A I Larkin, A quantum fluids approach to frustrated Heisenberg models. (2000)
- [7] M.H. Abasheer, Nano technology, Atrak, Cairo (2010).
- [8] M.M. Radio, Introduction to Nano technology and applications, Dar Daigle Publisher Bagdad. (2014)
- [9] P.A.M. Dirac .The Principles of Quantuum Mechanics (4th Ed.). Oxford University Press, oxford .(2011)
- [10] H.A. Shahatta, Nano technology and Human Future, Tayba Publisher, Cairo. (2011)
- [11] R.J. Chen, H.C. Choi, S. Bangsaruntip, E. Yenilmex, X. Tang, Q. Wang, Y.L. Chang, H. Dai: An investigation of the mechanisms of electrode sensing of protein adsorption on carbon nanotube devices, J. Am. Chem. Soc. 126, 1563–1568. (2004)
- [12] D. Srivastava, Co mputational nanotechnology of carbon nanotubes. In: Carbon Nanotubes, Science and Applications, ed. by M. Meyyappan CRC, Boca Raton, pp. 25–36. (2004)
- [13] W.G. van der Wiel, S. De Franceschi, J.M. Elzerman, T. Fujisawa, S. Tarucha, and L.P. Kouwenhoven, Electron transport through double quantum dots, Rev. Mod. Phys. 75, 1–22. (2003)
- [14] Anonymous, Microelectromechanical Systems: Advanced Materials and Fabrication Methods (National Academy Press, Washington,) NMAB-483. (1997)

- [15] M. Roukes, Nanoelectromechanical systems face the future, *Phys. World* **14**, 25–31. (2001)
- [16] J.C. Eloy, Status of the MEMS Industry (Yole Developpement, Lyon 2005ssa), presented at SPIE Photonics West, San Jose. (2005)
- [17] S. Lawrence, Nanotech grows up, *Technol. Rev.* **108**(6), 31.
- [18] R.P. Feynman: There's plenty of room at the bottom, *Eng. Sci.* **23**, 22–36 (1960), [http: www.zyvex.com/ nanotech/feynman.html](http://www.zyvex.com/nanotech/feynman.html). (2005)
- [19] Amato, Nanotechnology, <http://www.ostp.gov/nstc/html/iwgn/iwgn.public.brochure/welcome.htm>, or, <http://www.nsf.gov/home/crssprgm/nano/nsfnireports.htm>. (2000)
- [20] Anonymous. National Nanotechnology Initiative [http://www.ostp.gov/nstc/html/iwgn.Fy01budsuppl/nni.pdf](http://www.ostp.gov/nstc/html/iwgn/Fy01budsuppl/nni.pdf), or, <http://www.nsf.gov/home/crssprgm/nano/nsfnireports.htm>. (2000)
- [21] Anonymous, Towards a European Strategy for Nanotechnology European Commission Research Directorate General, Brussels. (2004)
- [22] Y. Bar-Cohen (Ed.), *Biomimetics – Biologically Inspired Technologies* CRC, Boca Raton. (2005)
- [23] A.C. Fluit and F.J. Schmitz // *Clin. Microbiol. Infect.* 10-272. (2004)
- [24] B.M. Babior // *Am. J. Med.* 109 -33 R.A. Miller and B.E. Britigan // *Clin. Microbiol. Rev.* 10-1 (1997). (2000).
- [25] W.D. Splettstoesser and P. Schuff-Werner // *Microsc. Res. Tech.* 57- 441. (2002)
- [26] R.A. Clark // *J. Infect. Dis.* 161-1. (1990)
- [27] I. Paspaltsis, K. Kotta, R. Lagoudaki, N. Grigoriadis, I. Poullos and T. Sklaviadis // *J. Gen. Virol.* 87 -3125-140. (2006)
- [28] J.C. Ireland, (1993) P. Klostermann, E.W. Rice and R.M. Clark // *Appl. Environ. Microbiol.* 59-1668 Titaniumdioxide photocatalysis, fundamentals and application on photoinactivation 125 Ireland. (1993)
- [29] V. Ramamurthy, *Organic Photochemistry* Taylor & Francis. (1997)
- [30] Attia AJ, Kadhim SH, Hussen FH. Photocatalytic degradation of textile dyeing wastewater using titanium dioxide and zinc oxide. *EJournal of Chemistry*, 5(2), 219-23. (2008)

- [31] M.J. Casteel, K. Jayaraj, A. Gold, L.M. Ball and M.D. Sobsey, *Photochem. Photobiol.* 80- 294. (2004)
- [32] J. Gamage and Z.S. Zhang, *Int. J. Photoenergy* Article ID 764870. (2010)
- [33] Y. Oka, W.C. Kim, T. Yoshida, T. Hirashima, H. Mouri, H. Urade, Y. Itoh and T. Kubo , *J. Biomed. Mater. Res. B* 86B 530. (2008)
- [34] R. Baan, K. Straif, Y. Grosse, B. Secretan, F. El Ghissassi and V. Coglianò, *Lancet Oncol.* 7-295 (2006).
- [35] V.L. Colvin.*Nat. Biotech.* 21 1166.L.Caballero, K.A. Whitehead, N.S. Allen and J. Verran, *J. Photoch. Photobio. A.* (2003)
276 -50. (2013)
- [36] T. Zuccheri, M. Colonna, I. Stefanini, C. Santini and D. Gioia *Materials* 6- 3270. (2013)
- [37] K.S. Yao, D.Y. Wang, C.Y. Chang, K.W. Weng, L.Y. Yang, S.J. Lee, T.C. Cheng and C.C. Hwang, *Surf. Coat. Technol.* 202-1329. (2007)
- [38] P.S.M. Dunlop, J.A. Byrne, N. Manga and B.R. Eggins, *J. Photoch. Photobio. A* 148-355. (2002)
- [39] R. Dillert, U. Siemon and D. Bahnemann, *Chem. Eng. Technol.* 21-356 (1998).
- [40] C.M.B. Carvalho, J.P.C. Tomé, M.A.F. Faustino, M.G.P.M.S. Neves, A.C. Tomé, J.A.S. Cavaleiro, L. Costa, E. Alves, A. Oliveira, Â. Cunha and A. Almeida , *J. Porphyrins Phthalocyanines* 13- 574. (2009)
- [41] Neppolian B, Choi HC, Sakthivel S, Arabindoo B, Murugesan V. Solar/UV-induced photocatalytic degradation of three commercial textile dyes. *Journal of Hazardous Materials*, 89(2-3), 303–17. (2002)
- [42] Sin J-C, Lam S-M, Mohamed AR, Lee K-T. Degrading endocrine disrupting chemicals from wastewater by TiO₂ photocatalysis: A review. *International Journal of Photoenergy*, 185159. (2012)
- [43] Nakata K, Fujishimaa A. TiO₂ photocatalysis: Design and applications. *Journal of Photochemistry and Photobiology C.Photochemistry Reviews*, 13(3), 169-89. (2012)

- [44] Vilar VJP, Gomes AIE, Ramos VM, Maldonado MI, Boaventura RAR. Solar photocatalysis of a recalcitrant coloured effluent from a wastewater treatment plant *Photochemical & Photobiological Sciences*, 8(5), 691-8. (2009)
- [45] Chong MN, Jin B, Chow CWK, Saint C. recent developments in photocatalytic water treatment technology: A review. *Water Research*, 44(10), 2997-3027. (2010)
- [46] Rizzo L, Meric S, Guida M, Kassinos D, Belgiorno V Heterogenous photocatalytic degradation kinetics and detoxification of an urban wastewater treatment plant effluent contaminated with pharmaceuticals. *Water Research*, 43(16), 4070–8.
- [47] Abhang RM, Kumar D, Taralkar SV Design of photocatalytic reactor for degradation of phenol in wastewater. *International Journal of Chemical Engineering and Applications*, 2(5), 337-41. (2011)
- [48] Ibadon AO, Fitzpatrick P Heterogeneous photocatalysis: Recent advances and applications. *Catalysts*, 3, 189-218. (2013)
- [49] Ni M, Leung MKH, Leung DYC, Sumathy K A review and recent developments in photocatalytic water-splitting using TiO₂ for hydrogen production. *Renewable and Sustainable Energy Reviews*, 11, 401–25. (2007)
- [50] Samanamud GRL, Loures CCA, Souza AL, Salazar RFS, Oliveira IS, Silva MB, et al Heterogeneous photocatalytic degradation of dairy wastewater using immobilized ZnO. *ISRN Chemical Engineering*, 275371, 1-8. (2012)
- [51] Homem V, Santos L Degradation and removal methods of antibiotics from aqueous matrices - A review. *Journal of Environmental Management*, 92(10), 2304-47. (2011)
- [52] Mondal K, Kumar J, Sharma A Self-organized macroporous thin carbon films for supported metal catalysis. *Colloids and Surfaces A: Physicochemical and Engineering Aspects*, 427, 83–94. (2013)
- [53] Mondal K, Kumar J, Sharma A TiO₂ nanoparticles impregnated photocatalytic macroporous carbon films by spin coating. *Nanomaterials and Energy*. (2013)

- [54] Rizzo L, Fiorentino A, Anselmo A Advanced treatment of urban wastewater by UV radiation: Effect on antibiotics and antibiotic-resistant E. coli strains. *Chemosphere*, 92(2), 171–6. (2013)
- [55] Priya SS, Premalatha M, Anantharaman N Solar photocatalytic treatment of phenolic wastewater-potential, challenges and opportunities. *ARPN Journal of Engineering and Applied Sciences*, 3(6), 36-41. (2008)
- [56] Chen X, Mao SS Titanium dioxide nanomaterials: Synthesis, properties, modifications, and applications. *Chemical Reviews* 107(7), 2891-959. (2007)
- [57] Attia AJ, Kadhim SH, Hussen FH Photocatalytic degradation of textile dyeing wastewater using titanium dioxide and zinc oxide. *EJournal of Chemistry*, 5(2), 219-23. (2008)
- [58] Akpan UG, Hameed BH Parameters affecting the photocatalytic degradation of dyes using TiO₂-based photocatalysts: A review. *Journal of Hazardous Materials* 170(2-3), 520-9. (2009)
- [59] Hussen FH, Abass TA Photocatalytic treatment of textile industrial wastewater. *International Journal of Chemical Science*, 8(3), 1353-64. (2010)
- [60] Asad S, Amoozegar MA, Pourbabae AA, Sarbolouki MN, Dastghei SMM Decolorization of textile azo dyes by newly isolated halophilic and halotolerant bacteria. *Bioresource Technology*, 98(11), 2082-8. (2007)
- [61] Ndasi NP, Augustin M, Bosco TJ Biodecolourisation of textile dyes by local microbial consortia isolated from dye polluted soils in Ngaoundere. *International Journal of Environmental Sciences*, 1(7), 1403-19. (2011)
- [62] Elahee K Heat recovery in the textile dyeing and finishing industry: lessons from developing economies *Journal of Energy in Southern Africa*, 21(3), 9-15. (2010)
- [63] M. RK, K.S Advanced treatment of textiles yarn dyeing waste water towards reuse using reverse osmosis membrane. *International Journal on Applied Bioengineering*, 4(1), 25-33. (2010)

- [64] Singh P, Mondal K, Sharma A Reusable electrospun mesoporous ZnO nanofiber mats for photocatalytic degradation of polycyclic aromatic hydrocarbon dyes in wastewater. *Journal of Colloid and Interface Science*, 394, 208-15. (2013)
- [65] Hoffmann MR, Martin ST, Choi W, Bahnemann DW Environmental Applications of Semiconductor Photocatalysis. *Chemical Reviews*, 95(1), 69-96. (1995)
- [66] Meng Z, Juan Z Wastewater treatment by photocatalytic oxidation of nano-ZnO. *Global Environmental Policy in Japan*, 12, 1-9. (2008)
- [67] Hernandez-Alonso MD, Fresno F, Suarez S, Coronado JM Development of alternative photocatalysts to TiO₂: Challenges and opportunities. *Energy & Environmental Science*, 2(12), 1231-57. (2009)
- [68] Vandevivere PC, Bianchi R, Verstraete W Treatment and reuse of wastewater from the textile wet-processing industry: Review of emerging technologies. *Journal of Chemical Technology and Biotechnology* 72(4), 289-302. (1998)
- [69] Chan YJ, Chong MF, Law CL, Hassell DG A review on anaerobic-aerobic treatment of industrial and municipal wastewater. *Chemical Engineering Journal*, 155(1-2), 1-18. (2009)
- [70] Swaminathan M, Muruganandham M, Sillanpaa M Advanced oxidation processes for wastewater treatment. *International Journal of Photoenergy*, 2013 (683682), 1-3. (2013)
- [71] Agustina TE, Ang HM, Vareek VK A review of synergistic effect of photocatalysis and ozonation on wastewater treatment. *Journal of Photochemistry and Photobiology C: Photochemistry Reviews*, 6(4), 264-73. (2005)
- [72] Rice RG. (2004) Applications of ozone for industrial wastewater treatment — A review. *Ozone-Science & Engineering: The Journal of the International Ozone Association* 1997; 18(6), 477-515.
- [73] Gogate PR, Pandit AB A review of imperative technologies for wastewater treatment II: hybrid methods. *Advances in Environmental Research*, 8(3-4), 553-97. (2004)

- [74] Wojnarovits L, Takacs E Irradiation treatment of azo dye containing wastewater: An overview. *Radiation Physics and Chemistry* 77(3), 225-44. (2008)
- [75] Azarian G, Mesdaghinia A, Vaezi F, Nabizadeh R, Nematollahi D Algae removal by electro-coagulation process, application for treatment of the effluent from an industrial wastewater treatment plant *Iranian Journal of Public Health* 36(4), 57-64. (2007)
- [76] Inan H, Dimoglo A, Simsek H, Karpuzcu M. Olive oil mill wastewater treatment by means of electro-coagulation. *Separation and Purification Technology*, 36(1), 23-31. (2004)
- [77] Arslan I, Balcioglu IA Advanced oxidation of raw and biotreated textile industry wastewater with O₃, H₂O₂/UV-C and their sequential application. *Journal of Chemical Technology and Biotechnology* 76, 53-60. (2001)
- [78] Lin SH, Chang CC Treatment of landfill leachate by combined electro-Fenton oxidation and sequencing batch reactor method. *Water Research* 34(17), 4243-9. (2000)
- [79] Jon P. Scott, Olli's DF Integration of chemical and biological oxidation processes for water treatment: Review and recommendations. *Environmental Progress* 14(2), 88-103. (1995)
- [80] Oller I, Malato S, Sánchez-Pérez JA Combination of Advanced Oxidation Processes and biological treatments for wastewater decontamination-A review. *Science of the Total Environment* 409(20), 4141-66. (2011)
- [81] Arsene D, Musteret CP, Catrinescu C, Apopei P, Barjoveanu G, Teodosiu C Combined oxidation and ultrafiltration processes for the removal of priority organic pollutants from wastewaters. *Environmental Engineering and Management Journal* 10(12), 1967-76. (2011)
- [82] Turchi CS, Ollis DF Photocatalytic degradation of organic water contaminants: Mechanisms involving hydroxyl radical attack. *Journal of Catalysis* 122(1), 178-92. (1990)

- [83] Veprek-Siska J, Lunak S Photocatalytic effects of trace metals evidence against a free radical chain mechanism in sulfite auto oxidation. *Reaction Kinetics and Catalysis Letters* 8(4), 483-7. (1978)
- [84] Ali R, Hassan SH Degradation studies on paraquat and Malathion using TiO₂/ZnO based photocatalyst. *The Malaysian Journal of Analytical Sciences* 12(1), 77-87. (2008)
- [85] Baruah S, Pal SK, Dutta J Nanostructured zinc oxide for water treatment. *Nanoscience & Nanotechnology-Asia* 2, 90-102. (2012)
- [86] Adams LK, Lyon DY, Alvarez PJ JComparative eco-toxicity of nanoscale TiO₂, SiO₂, and ZnO water suspensions. *Water Research* 40(19), 3527 – 32. (2006)
- [87] Sabin F, Türk T, Vogler ADecontamination of industrial waste water by photocatalytic oxidation of organic components: A model study. *Zeitschrift Fur Wasser-Und Abwasser-Forschung-Journal for Water and Wastewater Research-Acta Hydrochimica ET Hydrobiologica* 25(3), 163-7. (1992)
- [88] Mehrvar M, Anderson WA, Moo-Young M Photocatalytic degradation of aqueous organic solvents in the presence of hydroxyl radical scavengers. *International Journal of Photoenergy* 3, 187-91. (2001)
- [89] Khezrianjoo S, Revanasiddappa H Langmuir-Hinshelwood kinetic expression for the photocatalytic degradation of metanil yellow aqueous solutions by ZnO catalyst. *Chemical Sciences Journal* 2012(CSJ-85), 1-7. (2012)
- [90] IAVICOLI, V. LESO, L. FONTANA, A. BERGAMASCHI- Toxicological effects of titanium dioxide nanoparticles: a review of in vitro mammalian studies –European Review for Medical and Pharmacological Sciences 15, 481-508.(2011)
- . [91] Manoj A. Lazar, Shaji Varghese and Santhosh S. Nair Photocatalytic Water Treatment by Titanium Dioxide: Recent Updates/ Catalysts, 2, 572-601, doi, 10.3390/catal2040572catalystsISSN 2073-4344 www.mdpi.com/journal/catalysts. (2012)
- . [92] Clayton Wright¹, Anand Krishnan V. Iyer¹, Liying Wang², Nianqiang Wu³, Juan S. Yakisich¹, Yon Rojanasakul⁴, and Neelam Azad¹-Effects of titanium dioxide.

nanoparticles on human keratinocytes-Published in final edited form as: Drug Chem Toxicol. 2017 January, 40(1): 90–100. Doi.10.1080/01480545.1185111. (2016)

. [93] Karishma K. Chorawalaa, Mehali J. Mehtab/ Applications of Nanotechnology in Wastewater Treatment/ International Journal of Innovative and Emerging Research in Engineering Volume 2, Issue 1, .(2015)

[94] Javad Sharifi Rad^{1,2}, Mahsan Hoseini Alfatemi³, Mehdi Sharifi Rad^{4,5},Majid Sharifi Rad⁶, Dhrubo Jyoti Sen⁷ and Sasan Mohsenzadeh⁸/In-vivo Titanium Dioxide (TiO₂) Nanoparticles Effects on Chromosomal Abnormalities and Lactate Dehydrogenase Activity /American Journal of Advanced Drug Delivery www.ajadd.co.uk /AJADD[1][3] 232-237.(2013)

[95] Huo Q, Margolese D I and Stucky G D Science 267 865. (1995)

[96] Bever M.B, Encyclopedia of Mater. Sci. Eng, Pergamon, Oxford, 48739. (1986)

[97] Lampart C.M. and Granquist C.G. SPIE, Optical Engineering Press, Bellingham WA. (1990)

[98] Antonelli D M and Ying J Y (1995). Angew. Chem., Intl. Ed. Engl. 34. (2014)

[99] Richter J.H.: Electronic Properties of Metal Oxide Films Studied by Core Level Spectroscopy, DigitalComprehensive Summaries of Uppsala Faculty of Sci-ence.

[100] Patrick-Griffith, M. The origins of an important cactus crop, opuntia ficus-indica (cactaceae): New molecular evidence. Am. J. Bot. 91, 1915–19. (2004)